ISSN 0252-1075
Contribution from IITM
Research Report No. RR-098

# Thermodynamics and Dynamics of the Upper Ocean Mixed Layer in the Central and Eastern Arabian Sea

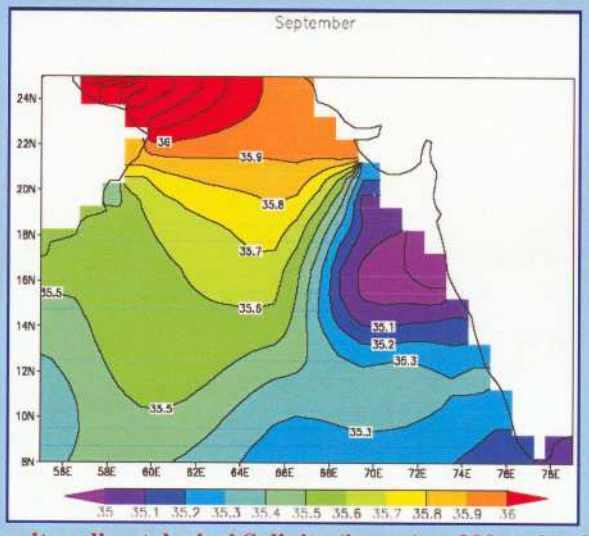


Levitus climatological Salinity (in psu) at 200 m depth

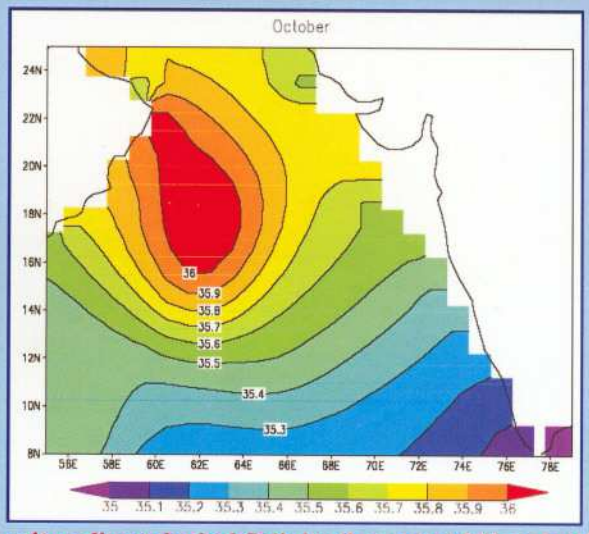


Levitus climatological Salinity (in psu) at 500 m depth

C. Gnanaseelan, A.K. Mishra, Bijoy Thompson
and
P.S. Salvekar

August 2003

Indian Institute of Tropical Meteorology
Pune - 411 008, India

ISSN 0252-1075
Contribution from IITM
Research Report No. RR-098

# Thermodynamics and Dynamics of the Upper Ocean Mixed Layer in the Central and Eastern Arabian Sea

C. Gnanaseelan, A.K.Mishra, Bijoy Thompson
and
P.S. Salvekar

August 2003

**Indian Institute of Tropical Meteorology**
Dr. Homi Bhabha Road, Pashan Pune - 411 008
Maharashtra, India

E-mail : lip@tropmet.ernet.in
Web : http://www.tropmet.ernet.in
Fax : 91-020-5893825
Telephone : 91-020-5893600

# CONTENTS



# Thermodynamics and Dynamics of the Upper Ocean Mixed Layer in the Central and Eastern Arabian Sea Part I: Observations and Analysis

**C. Gnanaseelan, A. K. Mishra, Bijoy Thompson, and P. S. Salvekar**

**Indian Institute of Tropical Meteorology**
**Dr. Homi Bhabha Road, Pashan**
**Pune-411008**

## ABSTRACT

Arabian Sea is considered to be a region of specific interest because of its association with monsoon in general and plays an important role in Indian summer monsoon in particular. Sea surface temperature over this sea varies from 23° C to 32° C from NE to SW monsoon. While sea surface salinity of the entire northern Arabian Sea north of 17° N ranges from 36.2 to 36.8 psu (ppt or parts per thousand) and south of 17° N it varies from 35 to 36.2 psu. Sea surface currents are caused by monsoonal winds, during southwest monsoon and they are clockwise, while during northeast monsoon they are anti-clockwise. Having associated with such higher variability this sea is still identified as one of the data sparse regions. However in the present study, data obtained from Woods Hole Oceanographic Institute (WHOI) mooring deployed at 15.5° N, 61.5° E for a period of one year (Oct. 1994 to Oct. 1995) and the deep sea mooring buoy (DS1, by National Institute of Ocean Technology (NIOT), Chennai, Department of Ocean Development (DOD), Government of India) located at 15.3° N, 69.3° E, for a period of almost an year (Feb. 1998 to Dec. 1998) were used for analysis and understanding the mixed layer variability and its thermodynamics of the central and eastern Arabian sea respectively. A well defined diurnal cycle appears to occur in the upper ocean because of intense seasonal solar heating. Although one year long data set is used for the study, special attention has been given to understand the processes associated with the 1995 southwest monsoon season. The study has revealed that the strong winds associated with the SW monsoon appear to have played an important role in the declining of the SST from a high value of 31° C to 25° C from before onset through onset of Monsoon (June) to the high peak phase of Monsoon (August) at WHOI Whereas the range variation of SST over the DS1 location is 30.6°C to 28.2°C. The lowest being observed in August and highest in May. However, the summer monsoon cooling from May to August at both the stations is 6°C (WHOI) and 2.4°C (DS1). The plausible reason for cooling of the ocean surface during the above period is observed to be due to the proximity of these stations to the climatological axis of the Findlater Jet during the south west monsoon season. Nevertheless, the DS1 location is comparatively far south to the axis of the above jet.

## 1. Introduction

Seasonal changes in atmospheric forcing subdivide the Arabian Sea into the southwest and northeast monsoon and two inter-monsoonal periods. These periods are of entirely different characteristics. The semiannual reversal of the winds is a special feature of the Arabian Sea. The annual march of the SST over most of the world ocean shows warming during the fair weather period of spring and summer and cooling during fall and winter. In contrast the Arabian Sea SST shows four phases; warming phase from February to May, cooling from May to August, warming from September to mid November and cooling from mid November to January (Shetye, 1986). The onset of the summer monsoon cools and deepens the mixed layer of the Arabian Sea with different magnitude. In fact in the Central Arabian Sea 4°-5° C cooling (INDEX, 1977) associated with the maximum deepening (60-80 m) of the mixed layer was observed around 10° N, 60° E (Rao, 1987). He also found that the mixed layer of the Central Arabian Sea cooled by 2°-3° C and deepened by 55 m with the onset and progress of the monsoon over the Indian subcontinent in the year 1977. He also concluded that the net surface heat loss is contributing 3-5 times more in cooling than that of entrainment. Although the observations by Rao (1986) and surface heat flux climatologies by Hastenrath & Lamb (1979 a, b) and by Oberhuber (1988) have suggested that the surface heat flux was negative (a net oceanic heat loss) which drive the convective entrainment and additional cooling, but the large scale budgets of the Arabian sea during the SW monsoon season showed that there is a net heat gain which probably be offset by horizontal advection and upwelling, leading to the net heat loss in the upper ocean layer (Duing and Leetma, 1980, Weller et al. 1998). It shows that the surface fluxes in the region and their important role in the mixed layer dynamics are still not completely understood.

It has been proved through several studies that there exists a very good relationship between SST anomalies and anomalies in monsoon rainfall over India. The variability of the SST over the Arabian Sea has been linked to the mean rainfall over India by a correlation study (Shukla and Mishra, 1977). In their study Shukla and Mishra (1977) found that the surface wind speed over the Central Arabian Sea, mean monthly SST and mean monthly rainfall over Central and Western India are very well linked with each other. In a GCM study Shukla (1975) has further shown that the warm anomalies of Arabian Sea SST results in higher precipitation over India. Although Raghavan et. al. (1978) questioned the validity of fixing time in an anomaly in the sea surface temperature which was done in Shukla's computations. Raghavan et. al. (1978), found that the anomalies are in fact short lived and episodes of strong and weak monsoon rainfall appear to coincide with the fluctuations of SST in the Western Arabian Sea on time scale as short as one week. In addition a good correlation has been found between the intensity of the East African low level jet and Indian rainfall (Findlater, 1969 and Saha, 1974).

Dube et. al. (1990) have studied the interannual variability of the ocean's upper layer thickness and surface wind stress curl over the central Arabian Sea. Due to the lack of oceanographic observational data over the Central Arabian Sea region Dube et. al. (1990) have used the output fields of an Indian Ocean Model (Luther and O'Brien, 1985) for their study. They found that a good correlation exists between thinner ocean upper layer with cooler surface waters and better (higher) Indian monsoon rainfall. So, majority of the scientific community now agree that the sea surface temperature, mixed layer temperature and the thickness of the mixed layer can play a significant role in

determining the intensity of monsoon rainfall and its temporal and spatial distributions over India. Several past studies reflect that SST over the Arabian Sea has been recognized as an important boundary condition which triggers the onset of the monsoon and the onset vortex. Singh (1998) found that mean sea level pressure (SLP) over the Arabian Sea (north of 5° N) during May, and the mean SST gradient over the Arabian Sea between 7.5° N and 17.5° N during May hold promise to become potential predictors for the Indian summer monsoon rainfall.

Ocean currents are the result of wind stress on the surface of the open ocean, driven by horizontal pressure gradients and differences in density as a result of variations in temperature and salinity. Based on their causative factors, ocean circulation can be classified mainly into two groups. They are: (1) wind driven circulation resulted due to the wind stress, and (2) thermohaline circulation which is due to the density changes normally occurs due to a change in salinity and/or temperature. During the SW monsoon season some peculiarities in the circulation of the water masses is already observed in the Arabian Sea, especially along the African coast. Bruce (1979), has observed the seasonal development of some large scale eddies which occur during the strong SW monsoon through series of temperature sections along the Tanker Sea lane off the east of African and Arabian coast. In the northern Somali basin a large 'prime eddy' is observed approximately between 4° N and 12° N almost every year. The horizontal dimensions of this eddy are 400 to 600 Km and it varies considerably during a single monsoon season. Observations have revealed that an eddy of relatively smaller horizontal dimension is also one of the interesting circulation features off Socotra between 12° N and 15° N. The Socotra eddy is mainly evident in July and August (Bruce, 1979). An eddy south of about 5°N and nearby the southern boundary of primary eddy and to the east African coast was also observed during some years. 'Prime eddy' is observed to be considerably larger and more energetic than the other eddies formed in the region. It was also observed that 'prime eddy' continues to remain in this location at least for three months after the complete withdrawal of the monsoon. It appears in the near surface water (0-100 m) in the late May or early June and continues to intensify until late September or early October (Bruce, 1979). By December eddies disappear; however, in some years the 'prime eddy' was found in the upper layer as late as January.

Observations indicated that the northwestward flowing alongshore current (Somali current) is clearly part of the eddy field found in each SW monsoon of the Somali coast. Each year the current diverges from the coast turning eastward about 9° N to 10° N, and during some years it turns at 3° N to 5° N forming a southern eddy. It is observed that the region where the strong coastal current turns offshore experiences the strong upwelling with reduced sea surface temperature as low as 13°C (Bruce, 1979). Therefore due to divergence of coastal currents strong upwelling occurs at 9° N to 11° N and in some years when southern eddy is formed the strong upwelling is also observed around 4° N to 6° N. During the MONEX (1979) observations period, Mahajan (1986) found that the satellite observed cloud free area off Somali coast persists throughout the monsoon season. The upwelled region has a crescent shape and a cold SST pattern that is mainly due to strong low level winds. In his study Mahajan (1986) also concluded that the upwelled cold water tends to encircle the eddy to mark its outer boundary. Due to the clockwise circulation of the eddy this upwelled cold water is then transported to offshore eastward. The volume transport of the prime eddy towards the east was found to be about 38 - 42 Sv (1 Sv = 1 Sverdrup $=10^6$ $m^3$ $s^{-1}$) for the upper layer from 0-400 dbar. The

volume transport for Socotra eddy found around 11-15° N is of the order of 9-15 Sv. Therefore there is clear indication of the cold water advection towards the eastern side of the African/Somali coast. The eastern extent of this transported cold water is still unknown and more observational evidence is required in this direction to make concrete conclusion.

Upper ocean response to diurnal variation of solar heating has a long research history. In the 1980's it has been realised that without a proper parameterization of diurnal scale of the solar heating and related upper ocean dynamics adequately, it is impossible to assess the seasonal and longer term mean temperature and mixed layer depth accurately (Woods, 1984). If we want to compute adequately the seasonal and long term temperature mixed layer depth in time scales of weeks, months, season or years, a successful parameterization of the diurnal solar heating at the sea surface is necessary. Generally, wind stress on the sea surface leads to turbulent mixing of upper ocean (30-60 m depth) and solar heating causes buoyancy effects (upwelling and sinking of warm and cold flumes of water). These forcings (wind and solar heating) will have an immediate consequence upon the sea surface temperature, surface heat fluxes and vertical water transport and try to modify them in the upper ocean environment. The above modification also tries to alter and activate the biological echo systems in upper ocean layers (Lee et. al. 2000).

In the present study an attempt has been made to investigate the diurnal and seasonal variations in the surface meteorological parameters and related mixed layer dynamics and thermodynamics. We selected two different observations in the Central Arabian Sea based on the one year data (from October 1994 to October 1995) observed by Woods Hole Oceanographic Institute (WHOI) mooring (hereafter we will call WHOI) and the data collected from the buoy deployed by the NIOT (DOD), Government of India, at 15.3° N, 69.3° E (hereafter we will refer the mooring as DS1) for the period 1 February 1998 to 31 December 1998. The above study further help us to understand the effect of monsoon circulation on the SST variability of the Arabian Sea.

## 2 Data and Methodology

### 2.1 Data and Observations

Data used in this study were the intensive buoy observations (hourly) at 15.5° N, 61.5° E (WHOI) during October 15, 1994 to October 20, 1995, deployed off the coast of Oman to collect the near surface meteorological and oceanic data and to prepare its time series and daily observed data of the deep sea buoy moored at 15.3° N, 69.3° E (DS1), NIOT (DOD) from February 1998 to December 1998. The details of the above experiments are given below.

**2.1.1 WHOI Mooring:** The surface buoy carried two separate, complete meteorological instrument packages and a third stand alone package that measured just humidity and air temperature. First set of instrument was Vector Averaging Wind Recorder (VAWR), recording every 7.5 minute and the other was the Improved Meteorological Recorder (IMET) recording every minute. The additional Rotronic MP-100 humidity and air temperature sensor was sampled by a third, independent or stand alone data logger. Further details about these sensors and their deployment are briefly in Weller et. al. (1998) and the references therein. It is important to mention that the WHOI

point considered here is close to the Findlater jet (climatological maximum in the wind speed) during south west monsoon (Findlater, 1969). Observable parameters were air temperature, relative humidity, specific humidity, rainfall rate, barometric pressure, wind velocity and direction, short wave radiation, long wave radiation, sea surface temperature and salinity, temperature and ocean currents at different depth in the ocean. Using the observations from IMET and VAWR sensors the best time series were selected. Further this data is averaged at one hour interval. More details of the preparation of the year long time series is described in Baumgartner et. al. (1997). Two separate moorings were deployed for the study of the two monsoons namely north-east monsoon-1994 and southwest monsoon-1995. The data observed by the second mooring which was deployed on the 22$^{nd}$ April 1995 is given more importance in this study for the detailed understanding of the oceans response during the SW monsoon-1995. Subsurface temperature measurements were made from the buoy and along the mooring line at 38 discrete depths ranging from 0.17 to 3025 m, four vector measuring current meters (VMCM) deployed deep (between 300 and 3025 m) providing temperature measurements. Salinity measurements were collected at 9 different discrete depths ranging from 1.42 to 250 m. Current measurements were collected at 9 discrete levels ranging from 5 to 750 m. The meteorological parameters like wind speed, wind direction, air temperature, precipitation and radiation were collected from the vector averaging wind recorder (VAWR) and the improved meteorological (IMET) system mounted on the Woods Hole Oceanographic Institution (WHOI) 3 m discus buoy. Using the observed temperature profile the mixed layer depth is estimated on the basis of the temperature difference (0.5 °C) criteria used by Levitus (1982) and Sprintall and Tomczak (1992). The instruments used at WHOI are discussed in Weller and Anderson (1996), and Weller et. al.(1998).

**2.1.2 DS1 Buoy:** The DS1 buoy data are daily data from February 1998 to December 1998 which contains the SST, Sea surface salinity, air temperature, barometric pressure and the components of the wind and current. SST, air temperature and wind speed are from the 3-hourly buoy observations. The buoy measured wind speed and air temperature at a height of 3.2 m and SST at a depth of 2.2 m, wind speed is extrapolated to 10 m height using a power law (Panofsky and Dutton, 1984). DS1 buoy was not equipped with radiation measuring instruments. The validity of the buoy data has already been studied in detail by Senan et. al. (2001), and the DS1 buoy data set were found satisfactory

2.2 Flux computation: The air-sea fluxes at WHOI were computed using version 2.5 of the bulk formulae developed during COARE, described in Fairall et. al. (1996). Shallowest (0.17 m) temperature observations were extrapolated to the surface to obtain a skin temperature which is then used for the flux computation. Net short-wave radiation was computed from incoming short-wave radiation using a variable albedo based on the solar elevation angle and an atmospheric transmittance of 0.720 (Payne, 1972). Net long wave radiation was computed by subtracting an estimate of the outgoing long-wave,

$$LW\uparrow = \varepsilon\sigma T^4 + (1-\varepsilon)LW\downarrow \qquad (1)$$

From the measured incoming longwave, LW↓, where the emmisivity ($\varepsilon$) was chosen to to be 0.97, and $\sigma$ is the Stefan-Boltzmann constant ($5.67 \times 10^{-8}$ W m$^{-2}$K$^{-4}$).

For the DS1 point latent and sensible heat flux were computed by using bulk aerodynamic formulas as described in Gnanaseelan et. al. (2001) and Gill (1982). The "bulk" formulas for sensible ($Q_s$) and latent ($Q_E$) heat fluxes involve drag (transfer) coefficients ($C_H$ for latent and $C_E$ for evaporative), the wind speed at a height of 10 meters ($U_{10}$), and the difference in temperature ('T' and humidity 'q') or water saturation (relative humidity, q), respectively.

The net heat flux can be expressed as the difference of net incoming and net outgoing heat, which can be represented as

$$Q_{net}=Q_{sw}-Q_{lw}-Q_s-Q_E \quad (2)$$

where $Q_{net}$ is Net Heat Flux (in Watt/m$^2$) , $Q_{sw}$ is short wave radiation (in Watt/m$^2$), $Q_{lw}$ is longwave radiation (in Watt/m$^2$). Each term of the Eq. (2) is as follows; Sensible heat

$$Q_s = \rho_{air}\, C_p\, C_H\, U_{10}\, (T_o - T_a) \quad (3)$$

and, Latent heat

$$Q_E = L\, \nu\, E = \rho_{air}\, L\, \nu\, C_E\, U_{10}\, (q_o - q_a). \quad (4)$$

where $C_p$ is the specific heat of air at constant pressure (1004 J Kg$^{-1}$K$^{-1}$), subscript "o" denotes ocean surface, and "a" denotes air, The best value for $C_H$ ranges from 0.83 x10$^{-3}$ (stable atmospheric conditions) to 1.10 x 10$^{-3}$ (unstable conditions). $C_E$ is estimated to be 1.5 x 10$^{-3}$. L is latent heat of vaporisation (2.495 x 10$^6$ J Kg$^{-1}$) and $\nu$ is 0.8.

Outgoing long-wave radiation (OLR) data on daily scale is interpolated at the DS1 point and then following relations (Shinoda et. al., 1998) were used to calculate the short wave and long wave radiations as done by Sengupta et. al. 2002.

$$Q_{sw} = 0.93\, OLR - 1.03 \quad (5)$$

where $Q_{sw}$ is short wave radiation in Watt/m$^2$ , similarly long wave radiation is evaluated using the relation

$$Q_{lw} = 0.985\sigma T_o^4 \left[0.39 - 0.05\{e_s(T_a)\}^{1/2}\right]\left(1 - 0.6n_c^2\right) + 4\left[0.985\sigma T_o^3\{T_o - T_a\}\right] \quad (6)$$

where $n_c$ is the cloud cover, which is estimated using the following relationship

$$n_c = 166.39 - 1.38OLR + 9.1(10^{-3})(OLR)^2 - 20.87(10^{-6})(OLR)^3$$

$\sigma$ is the Stefan-Boltzmann constant (5.67 x 10$^{-8}$ W m$^{-2}$ K$^{-4}$), $OLR$ is outgoing long wave radiation, $T_o$ is SST, $T_a$ air temperature and $e_s(T_a)$ is the vapor pressure of the atmosphere in mb, which can be calculated as below;

The wind stress ($\tau$) on the ocean surface can be calculated from the square of the wind speed (at a height of 10 meters; $U_{10}$), the density of air ($\rho_{air}$), and a drag coefficient ($C_D$) (Wu, 1982))

$$\tau = \rho_{air} C_{10} U_{10}^2 \quad (7)$$

the drag coefficient, $C_D$ is often represented by a constant.

The saturation specific humidity at the sea surface ($q_o$) and the specific humidity of the air near the sea surface ($q_a$) are estimated as

$$q_o = e_s(T_o) 0.622/P_A \quad (8)$$
$$q_a = e_s(T_a) 0.622/P_A \quad (9)$$

where $P_A$= atmospheric pressure, 0.622 is the ratio of the densities of the water vapour and dry air, and therefore we can get

$$e_s(T_o) = 10^{[9.4-(2353)/To]} \quad (10)$$
$$e_s(T_a) = 10^{[9.4-(2353)/Ta]} \quad (11)$$

## 3. Climatology

The monthly mean climatological SST at WHOI (Table 1) and DS1 (Table 2) is of bimodal type with a primary maximum in May-June (i. e. around 29° C at both points), a secondary maximum in October (27° C at WHOI and 28° C at DS1) (Hastenrath, 1979a). In response to the summer monsoonal forcing from June to August the sea surface at WHOI cools by 3.8° C. Similarly the wind speed of the former point infer that April month experiences less than 1 m/s while at the DS1 it is found to be greater than 3 m/s. From May onwards it appears to be increased to its peak, >15 m/s at WHOI and > 11 m/s at DS1 in the month of July. After attaining the maximum wind speed in July the wind again started decreasing to a minimum wind of speed 1-2 m/s and 3-4 m/s at WHOI and DS1 points respectively in October (see Table 1 and Table 2). Furthermore the air-sea interface flux climatology (Hastenrath, 1979b) shows high incoming SW (~ 260 W/m$^2$ at both points), net outgoing longwave around 60 W/m$^2$ resulting in net all wave 200 W/m$^2$ at WHOI and 190 W/m$^2$ at DS1. The mean monthly climatology of the net SW incoming radiation shows that the values are found to be decreased from April to July (Table 1 and 2). It is clear from the Tables that minimum value of the incoming net short-wave are in July (155 W/m$^2$ at WHOI and 150 W/m$^2$ at DS1). Thereafter it starts increasing slowly. Net incoming all wave radiation is also found to follow the same pattern, with a maximum 200 W/m$^2$ in April, minimum 118 W/m$^2$ in July at WHOI while at DS1, maximum 190 W/m$^2$ in April, and minimum 105 W/m$^2$ in July. After the onset of the monsoon in June, SST is found decreasing and therefore the computed sensible heat (from Atmosphere to ocean) are found maximum 13 W/m$^2$ at WHOI in August, in contrast to DS1 where the sensible heat (from Atmosphere to ocean) is found only 3 W/m$^2$ while in other months the DS1 point showed negligible sensible heat. Because of high wind speed the rate of evaporation are maximum 6.0 mm/day in the month of June and July at WHOI and 6.8 and 6.0 respectively at DS1, while it is 2.3 mm/day in April and 2.5 mm/day in September at WHOI. At DS1 the evaporation rate were found to be in the same trend, only magnitude differs in slightly. At WHOI the month of May, June and July are associated with latent heat (LH) flux more than 100 W/m$^2$, (112 W/m$^2$, 185

$W/m^2$ and 160 $W/m^2$ respectively in May, June and July). The July latent heat flux is found maximum. Similar variability of the latent heat flux is observed at the DS1 point.

The mean monthly net oceanic heat gain reveals that in the month of April and May the ocean at WHOI is receiving the energy from the atmosphere, i.e. 115 $W/m^2$ & 82 $W/m^2$ respectively (at DS1 it is 95 $W/m^2$ & 50 $W/m^2$) while in June and July ocean is loosing the heat 40 $W/m^2$ and 50 $W/m^2$ respectively. The net oceanic heat loss is more at DS1 (i.e. 80 $W/m^2$ in both June and July months) as compared to WHOI. This is because of high latent heat flux and low incoming short-wave radiation (SW) observed at DS1, due to local cloud development. Again in August and September almost 100 $W/m^2$ reductions in LH flux with respect to that of June imply that the net oceanic heat gain to positive value of 40 $W/m^2$ & 60 $W/m^2$ respectively at WHOI. Table-3 shows that the average air temperature for the SW monsoon season is 0.2° C higher at WHOI and 0.3° C higher at DS1 than the sea surface temperature. Similarly the sensible heat flux at WHOI for the season is relatively small but of positive sign (ocean gaining heat). The latent heat flux during the SW monsoon season increased initially with the wind speed but dropped to zero in July. On comparing the climatology of the two points we found that almost all the air-sea fluxes at both points are having the similar variability.

SST at the DS1 is 1° C higher in April with higher wind speed, and remained almost constant at 29° C upto June, although wind as well as other parameters were varying in the same way as at WHOI (except sensible heat). In April, May and June the 29° C SST shows the presence of climatological warm pool at DS1. At WHOI the SST is highest (29.2° C) in May and then with the onset of the monsoon it started decreasing from June onwards and SST was 25.2° C in August, implying that the sea surface cooled upto 4° C from May to August. SST climatology at DS1 depicts that the SST drops from and the minimum SST (27° C) is observed in August and September. It is important to note that drop in SST at WHOI during August is much more than that at DS1.

The climatology of the Arabian Sea at WHOI shows that during the monsoon season the positive curl of the wind stress enhances the upwelling. Especially, upwelling in the coastal area (along the western boundary of the Arabian Sea), brings up the cold water and then transports to offshore (Shetye, 1986). Since WHOI point is considerably far away from the coast and the observations are available only at the point of interest, it is very difficult to estimate the contribution of coastal upwelling and its associated advective effects in quantitative sense. Since the dynamics of the circulation off the Somalia have received considerable attention, sufficient literature and data are available for the analysis over Somalia region. But in contrast, very little is known about the rest of the basin. So at present it is very difficult to simulate the sea surface temperature of the Arabian Sea realistically during the SW monsoon season unless the thermodynamics and dynamics are known adequately (Shetye, 1986). Apart from the cold water advection the local entrainment and surface heat losses also cause the drop in the SST. But the WHOI observations revealed that the net heat flux to the ocean was positive (48 $W/m^2$ in June and 56 $W/m^2$ in July) during the SW monsoon-95 (Weller, 1998), which clearly indicates that the observed cooling is due to the local entrainment resulting to the mixed layer deepening and advection of cold water from the coast.

Figure (2) and (3) represent the T-S diagrams at WHOI and DS1 points respectively based on the Levitus (1994) climatological dataset. According to Sverdrup, a "water mass is defined by a segment of a T-S curve; in other words, a water mass is characterised by definite ranges of both temperature and salinity, where as "water type" is

frequently used to designate a body of water with fixed temperature and salinity. So according to definition a water type is depicted by a point on a T-S diagram whereas water mass may consist of a mixture of two or more water types. The water mass transport due to the currents at different levels is proved to be important in the Arabian Sea especially in the monsoon period.

The mass transport at the two observational points was studied using the above traditional T-S plots. The extreme cases were studied in detail. At the WHOI point, each diagram of Figure 2 depicts the T-S plots for a couple of months in pairs in sequence, from January to December. Upper left panel of Fig. 2 shows the plots for January (*) and February (o). Similarly, lower right panel of Fig. 2 shows the plots for November (*) and December (o). Nevertheless the remaining four figures follow the sequence in between the above two figures. Fig. 3 is same as Fig. 2, but for the DS1 station. In the above diagrams the abscissa depicts the salinity (in psu) and the ordinate depicts the potential temperature in degree celcius. The straight lines sloping upwards from left to right depicts the isopycnal (lines of equal density) also known as isopleths of density. The symbols plotted in figures depict the water mass characteristics at 19 standard depths (0, 10, 20, 30, 50, 75, 100. 125, 150, 200, 250, 300, 400, 500, 600, 700, 800, 900 and 1000 m). It is interesting to notice that at WHOI among the months, the October climatology has shown a sudden abrupt change in the curve with an increasing trend in salinity with depth from 125 m to 500 m. At 500 m depth the salinity has attained a maximum salinity of 36.0 psu. It is very difficult to assess the reason for a sudden occurrence of such high salinities between 125 to 500 m depth. In the top 20 m salinity is found increasing with depth in October month at WHOI point. Between 20 m and 100 m and at the three deeper levels (800, 900 and 1000 m) the salinities of September and October are same. The October climatology has shown a sudden transport of red sea water (RSW) at 500 m depth in to the point (Fig. 2) and region as well (see Fig. 4). In contrast at the DS1 point September climatology showed a transport of low salinity water at around 200 m depth. To understand the source of the water mass, the spatial distributions of water mass salinity are analysed. Figure 4 further strengthens our statement that at WHOI point; RSW is found around 500m depth. Figure 5 confirms that the low salinity water observed at DS1 around 200m is not from Bay of Bengal. It may be caused due to possible river discharge from the rivers Mandvi, Narmada and Tapti. Figure 6, the time-latitude and time-longitude sections further strengthen the source of low salinity water entering the region in September.

## 4.Results

To understand the complete variability of the mixed layer in diurnal and intra-seasonal scales, detailed analysis of the observed data is carried out in the present study. Figure 7 to Fig. 12 show the diurnal variation of the different fluxes and several oceanic and meteorological observable and estimated parameters for the months April to September 1995. The radiative fluxes are taken as follows: positive when the ocean is gaining and negative when atmosphere is gaining. Figure 7 shows the diurnal variation of (a) Net flux , (b) Mixed layer Depth, (c) Wind Speed (Ws) and wind direction (here the criteria of wind direction is towards this direction vide ref. Weller et.al.,1998) (Wd) and (d) Air temperature (Ta) and Sea Surface Temperature (To) at WHOI mooring during April 1995. Figure 8 to 12 show the same parameters similar to Figure 7(a to d) but for

May, June, July, August and September respectively. Net flux was found to oscillate across the average monthly value of 125 $W/m^2$ with daytime maxima and nighttime minima. Maxima in day time have reached upto a high value of 900 $W/m^2$ and a low value of 700 $W/m^2$, while due to radiational cooling during night time the net has flux reached upto -350 $W/m^2$ or less. Average value of the mixed layer depth for April at the WHOI point was 12 m, and it was found to vary between 5 m and 60 m. Diurnal variation in the wind speed was not very significant, mean monthly wind speed was 3 m/s and mean monthly wind direction was about 70 degrees. Air temperature for the April was found to oscillate across an average monthly value of 27.5° C, while an average SST in April 1995 was 28.5° C. It is seen that on an average SST was 1° C higher than the air temperature. Fig. 8 shows the diurnal variation of the above said parameters during May-1995. Average net flux for May was found reduced to 100 $W/m^2$. During day time heat flux was found to be between 700 $W/m^2$ and 825 $W/m^2$. The average MLD for the May was 23 m. Wind speed for the month of May was found varying between 9.5 m/s and 0.5 m/s with average value of 4.25 m/s. Diurnal plot of the Air temperature and SST are depicted in Fig. 8(d). Difference between average SST (29.8° C) and air temperature (29° C ) is still high. It is clear that during April and May the day time maxima in net flux appears to have reached a high value around 800 $W/m^2$ and during night time ocean is found to loose only around 200 $W/m^2$. The diurnal cycle of the wind is in phase with the MLD (see plot (b) & (c) of Fig. 7 and 8). Large diurnal variation of the MLD is observed in April. MLD was found to vary from 2 to 30 m in April. Significant diurnal variation in SST is also observed during April, which is a rare feature over the oceans. In Fig. 8, from 19$^{th}$ to 30$^{th}$ May, the wind speed was found weak (i.e. approx. 2 m/s) without diurnal variation, but noticeable diurnal cycle in the MLD (Fig. 8b) was observed which may be related to the varying wind directions seen in the observation. Thus the large diurnal variation in the SST observed in May is mainly due to the abnormal variation in the wind field and radiation, which in turn affect the MLD. In the beginning of May, SST was found to be around 30° C and started decreasing after 3$^{rd}$ May; this is mainly associated with the observed strong winds. The wind appears to have weakened after 17 May and continued upto 19$^{th}$ May and became constant at 2m/s during the rest of the period. Following this change in wind speed the SST started rising (inspite of large diurnal rain) quickly from 30° to 31° C during the same period from 17$^{th}$ May to 31$^{st}$ May.

Average net heat flux at the ocean surface in the month of June (Fig. 9) was about 50 $W/m^2$, which is one of the most striking features observed. Net flux peaks in the daytime was found to be oscillating between 500 $W/m^2$ and 800 $W/m^2$, while during nighttime it has varied from -200 to - 250 $W/m^2$. Average MLD was 45 m. The MLD was found to have 65 m maxima and 12 m minima. Initially, in the first half, the wind speed had increased and reached up to 12 m/s in the mid June. At the onset of the monsoon wind speed rose initially in early May, and then became light, before rising again in early June. Both the timings of rise in wind speed are well matching with that found by Fieux and Stommel (1977) for the multiple onset years. Year 1995 seems to be showing the characteristics of the multiple onset years. According to Faiux and Stommel (1977) multiple onset year is characterized by an early beginning of SW winds followed by a lull in the monsoon with partial failure of the winds and then resumption of full strength delayed until about 6$^{th}$ June. Based on the above mentioned criteria Weller (1998) accepted this year as a multiple onset year. In the second half consistent decrease in wind speed between 10 m/s and 15 m/s with negligible diurnal variation was observed. On an

average 10 m/s wind speed and 65 degree wind direction was observed. The SST was found to have decreased from about 30.75° C to 28.6° C for the first half of the month. The SST has remained constant during the second half of June. This type of steep decrease in the SST after the onset of the SW monsoon was also reported by Rao (1987). Although monsoon induced cooling has affected the air and sea temperatures, still on an average SST were observed to be 0.05° C higher than air temperature. Mixed layer depth and wind speed showed similar trend upto mid June. There after an opposite trend. There were no incidence of precipitation observed in June and the high wind speed has initiated the mixing process, which resulted in increasing MLD. Fig. 10 shows the diurnal variation of the same parameters for the month of July. The net flux was found to have oscillated across the average monthly value of approximately 60 $W/m^2$ with daytime maxima and nighttime minima. Maxima in day time reached upto maximum value of 825 $W/m^2$ and minimum value of 700 $W/m^2$, while due to radiational cooling during night time the net flux reached upto -250 $W/m^2$ or less. Average value of the mixed layer depth for July at the WHOI point was 65 m, and it was found to vary between 30 m and 90 m. Mean monthly wind speed was 12.5 m/s, and mean monthly wind direction was towards 54 degrees. Previous months decreasing trend in SST and air temperature was continued in July also. They have reached to 25.25° C and 26° C respectively. Air temperature for the July was found oscillating across the average monthly value of 27.4° C, while average SST in July 1995 was 26.8° C. However, in this month the average SST was 0.6° C lower than the air temperature. The reductions in the net heat flux in July are explained by analyzing different components of the air-sea fluxes. Increased wind speed had increased the rate of evaporation and therefore the latent heat (LH) flux which infact has negatively contributing to the net heat flux. Similarly the presence of clouds could also reduce the incoming radiation. The previous observations and model studies also showed that the month of July is associated with the strongest winds, high evaporation rate and cloudy sky. It is important to note that the air temperature (AT) is greater than SST in July, while the SST is found greater than AT in the other months. In mid July wind speed was found increasing up to 16-17 m/s, climatologically it is the seasonal as well as annual maximum value, again decreased to 9 m/s towards the end of the month. Wind direction was found almost steady towards 55 degrees. Significant SST reduction by almost 3° C (May to July) and deepening of MLD were observed in July.

Figure 11a shows that the net flux was varying between -125 $W/m^2$ and 820 $W/m^2$ with an average monthly value of 130 $W/m^2$ approximately. Wind speed in August has varied between 7 m/s and 10 m/s with relatively steady wind direction. The average mixed layer depth for the month of August was 35 m with diurnal variation ranging from 15 m to 60 m. Air temperature was constant with average 26.5° C, average SST for the August was 26° C, still lower than air temperature. But SST was found increasing with the advance of the month, average SST for the August was 26° C, still lower than the air temperature. The month of September is characterized by the withdrawal of the south west monsoon from the entire Indian subcontinent. Average net flux for the September was 125 $W/m^2$, average MLD was 32 m, mean monthly wind speed was approximately 7 m/s with the average wind direction of 70 degree (Fig. 12). The temperature of the sea surface is now found to increase rapidly. The monthly mean value (27.5° C) is 0.3° C higher than air temperature. There exists two significant bad weather periods during September. The first period corresponds to 11$^{th}$ September and the second period

corresponds to 18th September. On both these days the air temperatures seems to have fallen to 23.75 °C and 24.5 °C respectively. The reason for the sudden fall of the above air temperatures is observed to have occurred following an event of rainfall spell in the wake of convective clouds. It has been observed that on both these occasions the day time net heat flux and wind speed have decreased substantially as compared to the immediate neighboring days due to the possible presence of cloud. The plausible reason for the fall in wind speed is found to be due to an increase in pressure field on these days. Here, one can anticipate a horizontally moving surface pressure wave (vide Fig. 2 of Weller et. al., 1998). It is further found that the MLD appears to have decreased during following consecutive days a rise in SST, on corresponding rise in net radiation and associated week wind speed.

## 5.Discussions

In the foregoing section we have described some significant salient features on a diurnal, synoptic and monthly time scale. It has been observed that the upper ocean seem to have affected month after month due to the variation of surface meteorological fields with the growing monsoon conditions. It is not yet clearly known to what extent the upper ocean has responded to the ongoing activities of the immediate neighbor, i.e. the atmosphere near the WHOI buoy. To understand the transport of mass and heat in the different layers of the upper ocean water column, the monthly mean current and temperature profiles upto 100 m are analyzed in detail. Fig. 13 (a)-(f), shows the above monthly mean current and temperature profiles at 15.5° N, 61.5° E from April-1995 to September-1995. For the months of April and May (Fig. 13a, continuous line) the mean monthly current speed was small. In top 50 m the current was close to 5 cm/s. In April the surface current was found eastward, while at 10 m depth the water transport was from west south-west (approximately 62° from true north). It was from west to east in 20 m to 50 m below that relatively stronger current at around 65 m was observed (west North West). April SST was around 28.5° C and the MLD was approximately 18 m (Fig. 13c, continuous line). May current below 20 m depth was almost constant (5 cm/s), however the direction changed drastically.

May current profile strengthens the role of Ekman drift in the surface upto 40 m (Fig. 13a, dotted line). Due to the strong winds in June (Fig. 9) the Ekman current (drift) (i.e. Surface current direction is approximately 45° right from the wind direction in NH) was observed at the surface. It is a clear indication that the currents are dominated by Ekman drift during this period. In the top 40 m the currents were found decreasing with depth but the direction was almost constant at around 110° from true north (i.e. East south eastward current). In July (Fig. 10) the mean monthly south westerly winds of considerably larger speed (12.37 m/s) was observed. Average currents at each level were 2.5 times of the June currents (Fig. 13d). Strongest wind supported the Ekman drift, which resulted in the surface current of 40 cm/s flowing from west to east. During July the current direction (Fig. 13e) in the top 100 m was almost constant (eastward). Coastal upwelling along the coast of Oman and the cold water upwelling in the Socotra eddy region and its possible advection may be contributing a bit in July cooling (Figures not shown). High wind speed of July (Fig. 10) has supported the wind mixing in the mixed layer which resulted in deepening and cooling due to the entrainment of the cold water in the mixed layer. Strong currents in the upper layer can bring the cold water towards the

point of observation which will result in the cooling of the mixed layer. Mixed layer was found upto 65-70 m deep in this month with the SST of about 27° C which is around 1° C less than June SST (Fig. 13c, f). Since the under water currents at DS1 were not observed, it is of no use to discuss the possible mass and heat transport at DS1 during the observation period.

The physical processes controlling the SST in August (Fig. 11 d) attracts its own importance. Eventhough the wind speed (Fig. 11c) was reduced to 9.33 m/s but still strong enough to stir the ocean. Ekman component of the current is found to be very weak in this month (Fig. 13d). Current profile of the month of August (Fig. 13d) reveal that the strongest surface current of 55 cm/s eastward (Fig. 13e) was observed at the surface, the current was found decreasing with depth but maximum currents speed is found during this month at all levels, the direction of the current was almost constant around 140° from true north (i.e. southeastward). In August (Fig. 12f) SST reduced by 1° C, while the mixed layer depth shallowed (approximately 32 m). Since mixed layer shoaled in this month, SST cooling is not due to wind mixing but only due to advection. The speculation attracts much attention when we found that the August (Fig. 5) current was also favoring the cold water entering the region from the coast of Oman. However, some more observational evidence is essential to conclude the role of advection. In September with the retreat of the monsoon winds (Fig. 12c) were decreased to a low value of 6.82 m/s coming from SW, current (Fig. 13d) was decreased to around 20 cm/s at the surface and the direction (Fig. 13e) of the current was less than 50° from true north (i.e. coming from SSW). Fig. 13 comprises the daily mean plots of the air-sea interface transfer fluxes at WHOI for the monsoon season (i.e. 153 days starting from 1$^{st}$ April to 2$^{nd}$ September). This Figure has clearly shown that with the onset of the southwest monsoon, the short wave radiation reduced, which may be due to the possible presence of clouds (Weller et. al., 1998) over the observation point. Although the other fluxes are also contributing towards the net heat flux (Fig. 14) the short wave radiative flux is found to have controlled the net heat flux (dotted curve) during the monsoon season. Steep decrease in net flux on around 15$^{th}$ June, 22$^{nd}$ July and around 12$^{th}$ August was in phase with that in short wave radiation. Similarly peaks of the both fluxes on 23$^{rd}$ June, 12$^{th}$ July, 18$^{th}$ July and 10$^{th}$ August are also due to the short wave radiation. Since latent heat loss and the effective long wave radiation over the ocean are reduced during the monsoon season and found varying between 50 and 100 W/m$^2$ and around 50 W/m$^2$ respectively, therefore only short wave flux henceforth is controlling the net flux.

Further Fig. 15 shows the mean monthly sea surface temperature, net heat flux, sensible heat flux and latent heat flux at the point WHOI buoy with the available climatology from different sources. The only variable that almost all the climatologies could match well is sea surface temperature (Fig. 15a), however, the NCEP (Reynolds, 1998) SST (SST OI V2) is very well matching with the observations for all the months. Net heat flux at the point (Fig. 15b) was compared with that of Oberhuber (OBH) climatology and Southampton Oceanographic Center (SOC) climatology. It was found that OBH climatology was quite low for the entire monsoon season, while SOC values were in good agreement, except in the month of August where it was very low as compared to the observation. Sensible heat flux at the point is very well matching with the climatology, except during monsoon season, the climatology estimated from the Florida State University data set (1960-1980) and SOC climatology is not in good agreement during monsoon season, however, the OBH is well matching (Fig. 14c).

Similarly the latent heat flux is also compared with the FSU, OBH, SOC climatologies but none of them could reproduce as the observed high peaks of around 200 $W/m^2$ in the month of December and the low value of 70 $W/m^2$ in August. It shows that none of the climatology is in good agreement with the observation. Weller et. al. (1998) suspected that the year 1995 was a typical monsoon year in terms of its heat exchange and wind stress forcing, but due to limited availability of such data the fact is not verified. Fig. 15 shows the time depth variation of Levitus (1994) monthly climatology and observed temperature and salinity and found that the observed temperature profile at the point is well comparable with the Levitus, 1994 (a,b), but salinity profile was not in good agreement. It is important to note that the Levitus climatology is the latest and it is available at finer resolution exactly (1 ° x 1°), which is comparable with the observations (grid is coinciding with the observation point). Thus one can conclude that none of the climatology could give the real picture in this part of the ocean, especially the fluxes are most difficult to reproduce. Although, our study confines to observation points only (Fig. 1), and the climatology which is compared is linearly interpolated from the available grid, the chances of errors can not be ruled out, but still the variation is too large to be discussed on this ground. So a better climatology for this region is still required. The study shows that the old climatologies are loosing their significance and climatologies based on the data of recent years are very much essential for better understanding of the climate.

Figure 17 shows the SST and the flux computed at the DS1 location. Observed Sea surface temperature at DS1 is in good agreement with the NCEP (Reynolds, OI, version 2, data of 1998). SST (Fig. 17a) climatologies like FSU and OHB are not well matching with the DS1 observations. On the other hand Fig. 14 shows that the same climatologies were in close agreement with the WHOI observed SST. NCEP concurrent data is very well matching at both points. Validation of SST and wind speed observed at the DS1 using TRMM data has already been done by Senan et. al. (2001), but older climatologies are not matching with the observations. Thus one can easily come to conclude that the warm pool region of the eastern Arabian Sea is warmer than the climatology throughout the year. Different components of the heat fluxes are estimated using the formulae discussed earlier. It is observed from the Fig. 17 (b-d) that all climatologies are well matching among them, but none of them was found capable enough to match with the observation throughout the year.

Geographically WHOI and DS1 buoy points are falling on the same latitudinal belt, however, the longitudes and the period of observations are differed. Fig. 18 shows the mean monthly (a) SST (°C), (b) wind Speed (m/s), (c) barometric pressure (mb) and (d) air temperature (°C), at both WHOI and DS1 buoy points. Fig. 19 depicts the comparative plots of mean monthly (a) zonal wind (m/s), (b) meridional wind (m/s), (c) and (d) zonal and meridional currents (in cm/s) respectively at the above same points. As discussed earlier air-sea flux climatology of the points (Table-1 and Table 2) show almost similar variability during April to October. e.g. both the points are attaining maximum. As it is clear in the Fig 17 that the abrupt termination of spring warming (Sengupta et. al. 2002) at Arabian Sea DS1 buoy in late May and early June is due to the passage of the Tropical Cyclone 03A and 02A (Climate Diagnostic Bulletin of India, IMD, New Delhi) close to the position of the buoy. Similar changes in the wind speeds and the surface currents were also observed with the appearance of the cyclonic disturbance.

## 6. Conclusion

In the context of the Indian summer monsoon one question is often asked: "How important is the initial state of Indian Seas, particularly of the Arabian Sea, for the subsequent Monsoon?" The present study was an attempt to understand the importance and physical processes occurring in the region using the available data sets. The study reveals that wind speed is the controlling parameter of the mixed layer depth, both on diurnal scale and monthly scale. The wind directions are also equally important in determining the mixed layer depth. In most of the cases the frequent changes in wind direction was the reason for increase in the mixed layer depth and its significant diurnal variability associated with less wind speed was observed in many occasions. Different climatologies were compared with the observed data and it was found that year 1995 was a typical southwest monsoon season in terms of the onset, heat exchange strength and different wind forcing during the two monsoons. In the first week of May wind speed was found to increase and the direction has changed to southwesterly. On 18$^{th}$ May the winds were reduced to the magnitude 2-4 m/s after attaining the speed of 9m/s on 15$^{th}$ May. Wind directions were also found changing between 50 degrees and 175 degrees. Afterward, in first week of June wind started increasing gradually and reached to more than 10 m/s on 9$^{th}$ June accordingly the wind direction had also changed to southwesterly. The year 1995 was a multiple onset year with an early onset (around 10$^{th}$ May) followed by a lull (after 18$^{th}$ May) and then resumption of second monsoon onset to its full strength on 9$^{th}$ June. Strong advective currents in August is found to be responsible for bringing cold water mass in the region and resulting strong SST cooling. Also in August Ekman component of the current is found weakening, which was strong in May, June and July. The SST in the region warms by 3-4° C in the spring season, (April May). Surface and subsurface observations in the WHOI show a net surface heat loss of about 100 W/m$^2$ in spring with SST rising 4° C from mid February to mid May. Upper ocean processes in spring are primarily found to be one-dimensional with the warming being a response to surface heat flux minus penetrative radiation flux. However, the oceanic processes during the southwest monsoon are found to be more complex and more observations are essential for understanding the processes in detail. The DS1 observations were analysed mainly to compare with the WHOI, as they are incidentally fallen on the same latitude. This study further stresses that the eastern Arabian Sea (near DS1) is highly warmer throughout the year during 1998as compared to the normal monthly SST (Fig. 17a). Although the above result s true and confined to only one-year observation, it is too early to come to a conclusion that this warming phenomenon repeat every year. Therefore further studies on the mixed layer physics using more available marine meteorological data of NIOT buoys are required to be analysed to see weather the above warming phenomena is occur in other years also.

## 7. Acknowledgment

We thank Director, IITM for providing the infrastructure required for the study. The authors acknowledge R. A. Weller, T. D. Dickey and J. Marra for providing the meteorological and oceanographic data at WHOI point and wish to acknowledge NIOT, Chennai (DOD) for the DS1 buoy data. The authors acknowledge D. Sengupta and B. N.

Goswami, IISc, Bangalore for fruitful scientific discussions during the preparation of this report. We deeply acknowledge Shri P. Seetaramayya for the peer review of this report. Department of Science & Technology, Government of India provided the financial assistance through ICRP project (ES/48/004/99).

## 8. References

1.Bruce, J.G., 1979: Eddies off the Somali Coast During the Southwest Monsoon. J. Geophys. Res. 84, 7742-7748 Bruce (1979)

2.Baumgartner, M. F., Brink, M. J., Ostorm W. M., Trask, R. P., Weller, R. A., 1997: Arabian Sea Mixed Layer Dynamics Experiment Data Report, Upper Ocean Processes Group Technical Report 97-3, WHOI-97-08, Woods Hole Oceanographic Institution, Woods Hole, MA, USA, 02543, 169 pages.

3.Dube, S. K., Luther, M.E. And O'Brien, J. J., 1990: Relationship between Interannual variability in the Arabian Sea and India summer monsoon rainfall. Met. & Atmo. Phys., 44, 1- 4, 153-165.

4.Duing, W. and Leetma, A., 1980: Arabian Sea cooling: A preliminary heat budget, J. Phys. Oceano., 10, 307-312.

5.Fairall, C. W. Bradley, E. F., Rogers, D. P., Edson, J. B., Young G. S., 1996: Bulk Parameterization of Air-sea fluxes for TOGA COARE. J. Geophys. Res., 101, 3747-3764.

6.Fieux, M., H. Stommel, 1977: Onset of the Southwest monsoon over the Arabian Sea from marine reports of surface winds. Mon. Weath. Rev., 105, 231-236.

7.Findlater J., 1969: A major low-level air current near the Indian ocean during the Northern Summer. Quart. J. Roy. Met. Soc. , 95, 362-380.

8.Gill, A. E. , 1982: Atmosphere and Ocean Dynamics, Academic Press, New York.

9.Gnanaseelan, C, D.W. Ganer, K. Annapurnaiah, A. A. Deo & P.S. Salvekar, 2001: Seasonal heat transport in the North Indian Ocean during two contrasting monsoons. J. Ind. Geophys. Union, 5(1), 51-56.

10.Hastenrath, S., and Lamb P. J., 1979a: Climatic Atlas of the Indian Ocean, Part I, Surface Climate and Atmospheric Circulation, University of Wisconsin Press, Madison, 116pp

11.Hastenrath, S., and P. J. Lamb, P. J., 1979b: Climatic Atlas of the Indian Ocean, Part 2, The Oceanic Heat Budget, University of Wisconsin Press, Madison, 110pp

12.INDEX, 1977: An oceanographic contribution to international progress in the monsoon region of the Indian Ocean, Report No. ID, 075-01571, NSF, Washington, D. C.

13.Lee, C. M., B. H. Jones, K. H. Brink and A. S. Fischer, 2000: The upper-ocean response to monsoonal forcing in the Arabian Sea: seasonal and spatial variability, Deep Sea Research II, 47, 1177-1226.

14.Levitus, S, 1982: Climatological Atlas of the World Ocean NOAA Professional Paper 13, U. S. Government Printing Office, Washington D.C., 173pp.

15.Levitus S., R. Burgett and T.P. Boyer, 1994a: World Ocean Atlas 1994, Volume 3 : Salinity. NOAA Atlas NESDIS 3. 99pp.

16.Levitus S. and T.P. Boyer, 1994b: World Ocean Atlas 1994, Volume 4 : Temperature, NOAA Atlas NESDIS 4 11pp

17.Luther, M. E. and O'Brien J. J., 1985: A model of the seasonal circulation in the Arabian Sea forced by observed winds, Prog. in Oceano., 14, 353-385.
18.Mahajan, P. N., 1986: Satellite -observed upwelled region and prime eddy off Somali coast during Monex-79. Proc. Indian Acad. Sci. (Earth Planet. Sci.), 96, 41-47.
19.Oberhuber, J. M., 1988: An atlas based on `COADS' data set, Tech. Rep. 15, Max-Planck-Institute for Meteorology, 1988.
20.Panofsky, H. A. and J. A. Dutton, 2001: Atmospheric Turbulence, John Willey and Sons, New York, 397.
21.Payne, R. E., 1972: Albedo of the Sea surface. J. Atmos. Sci., 29, 959-970.
22.Raghavan et. al. 1978: Interaction between the west Arabian Sea and the Indian Monsoon, Mon. Weather. Rev., 106, 719-724.
23.Rao, R. R., 1987: The observed variability of the cooling and deepening of the mixed layer in the Central Arabian Sea during Monsoon: 77. Mausam, 38(1), 43-48.
24.Saha, K. R., 1974: Some aspects of the Arabian Sea summer monsoon, Tellus, 26, 464-476.
25.Senan, R., D. S. Anitha, and D. Sengupta, 2001: Validation of SST and wind speed from TRMM using north Indian Ocean moored buoy observations. CAOS Report 2001AS1. Centre for Atmospheric and Oceanic Sciences, Indian Institute of Science, Bangalore.
26.Sengupta, D., Ray, P. K. and Bhatt, G. S., 2002: Spring warming of the eastern Arabian Sea and Bay of bengal from buoy data. Geophys. Res. Lett., 29, 24-1-4.
27.Shetye, S. R. 1986: A model study of the seasonal cycle of the Arabian Sea surface temperature, J. Mar. Res., 44, 521-542.
28.Shinoda, T, Hendon, H. H., Glick J., 1998: Intraseasonal variability of Surface fluxes and sea surface temperature in the Tropical western Pacific and Indian Oceans. J. of Climate, 11, 1685-1702.
29.Shukla, J., 1975: Effect of Arabian sea-surface temperature anomaly on Indian summer monsoon: A numerical experiment with GFDL model. J. Atmos. Sci., 32, 503-511.
30.Shukla, J and Mishra B.M., 1977: Relationships between sea surface temperature and wind speed over the Central Arabia Sea, and monsoon rainfall over India. Mon. Wea. Rev., 105, 998-1002.
31.Singh, O. P., 1998: The association between the North Indian Ocean and summer monsoon rainfall over India. Mausam, 49, 325-330.
32.Sprintall, J. and Tomczak, M., 1992: Evidence of the barrier layer in the surface layer of the tropics. J. Geophys. Res., 97(C5), 7305-7316.
33.Weller, R. A., Anderson, S. P., 1996: Surface meteorology and air-sea fluxes in the western equatorial Pacific warm pool during TOGA coupled Ocean-Atmospheric Response Experiment, J. of Climate., 9, 1959-1990.
34.Weller, R. A., Baumgartner, M. F., Josey, S. A., Fischer, A. S., Kindle, J. C., 1998: Atmospheric forcing in the Arabian Sea during 1994-1995 observations and comparisons with climatology models. Deep Sea Research II, 45 (11), 1961-1999.
35.Woods, (1984), Ed. J. Houghtn, Cambridge University Press, 141.
36.Wu, J., 1982: Wind-Stress Coefficients Over Sea Surface from Breeze to Hurricane, J. Geophys. Res. 87, 9704.

**Table -1:** Climatological ( Hastenrath, 1979 (b)) Surface Heat fluxes at WHOI (15.5° N, 61.5° E) - Prepared from the Atlas

| Month | Fluxes at 15.5° N 61.5° E | | | | | | | SST | Wind |
|---|---|---|---|---|---|---|---|---|---|
| | Net (SW↓↑) ($W/m^2$) (i) | Net (LW↑↓) ($W/m^2$) (ii) | Net All wave ($W/m^2$) (i)-(ii) | Sensible Heat ($W/m^2$) | Latent Heat ($W/m^2$) | Evapor-ation (in mm $H_2O$/day) | Net Heat-Gain ($W/m^2$) | (°C) | Speed (m/s |
| April | 260 | 60 | 200 | 0 | -80 | 2.3 | 115 | 28 | <1 |
| May | 245 | - | 184 | 0 | -112 | 3.8 | 82 | 29.2 | 3-4 |
| June | 178 | - | 135 | 2 | -185 | 6.0 | -40 | 28.4 | 11-12 |
| July | 155 | 38 | 118 | 9 | -160 | 6.0 | -50 | 26.2 | >15 |
| August | 185 | - | 130 | 13 | -95 | 3.3 | 40 | 25.2 | 11-12 |
| Sept. | 180 | - | 135 | 5 | -80 | 2.5 | 60 | 25.6 | 6-7 |
| Oct. | 220 | 55 | 150 | 0 | -80 | 2.8 | 70 | 27.4 | 1-2 |

**Table -2:** Climatological ( Hastenrath, 1979 ( b ) ) Surface Heat fluxes at DS1 (15.3° N, 69.3° E) - Prepared from the Atlas

| Month | Fluxes at 15.3° N 69.3° E | | | | | | | SST (°C) | Wind Speed (m/s) |
|---|---|---|---|---|---|---|---|---|---|
| | Net (SW↓↑) ($W/m^2$) (i) | Net (LW↑↓) ($W/m^2$) (ii) | Net All wave ($W/m^2$) (i)-(ii) | Sensible Heat ($W/m^2$) | Latent Heat ($W/m^2$) | Evapor-ation (in mm $H_2O$/day) | Net Heat-Gain ($W/m^2$) | | |
| April | 260 | 57 | 190 | 0 | -80 | 3.1 | 95 | 28.9 | >3 |
| May | 230 | - | 168 | 0 | -118 | 4 | 50 | 29 | 3-4 |
| June | 160 | - | 118 | 0 | -190 | 6.8 | -80 | 29.1 | 8-9 |
| July | 150 | 34 | 105 | 0 | -160 | 6.0 | -80 | 28.1 | >11 |
| August | 160 | - | 120 | 3 | -120 | 4 | 0 | 27 | 8-9 |
| Sept. | 185 | - | 125 | 0 | -80 | 3 | 40 | 27 | 5 |
| Oct. | 198 | 49 | 135 | 0 | -80 | 3 | 40 | 28 | 3-4 |

( ↓↑=incoming -outgoing, ↑↓=outgoing- incoming)

**Table-3** Average value of observables and air-sea fluxes during SW monsoon (June- September)

| Parameter | Wind | | Temperature | | Heat Flux ($Watt/m^2$) | | | | |
|---|---|---|---|---|---|---|---|---|---|
| Experiments | Speed (m/s) | Direct. (deg.) | Air (°C) | SST (°C) | SH | LH | SW (net) | LW (net) | Net Flux |
| WHOI -1995 | 10.16 | 57 | 27.54 | 27.34 | 5.3 | -110 | 220.2 | -26 | 89.5 |
| DS1-1998 | 7.52 | - | 28.98 | 28.65 | 4.6 | -148 | 222.8 | -22.8 | 56.5 |

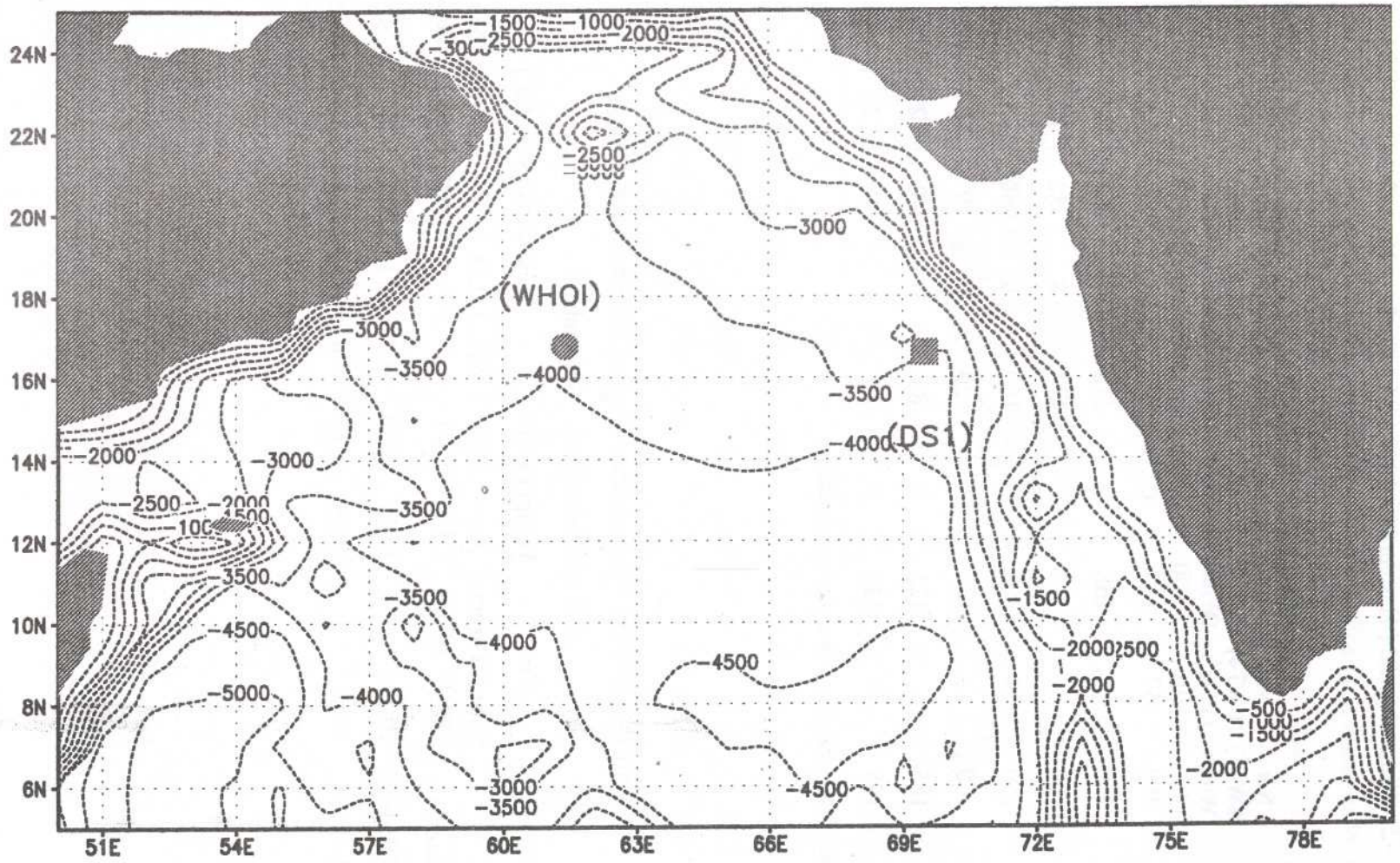


Fig. 1: Location Map (dashed lines are depth contour from ocean surface)

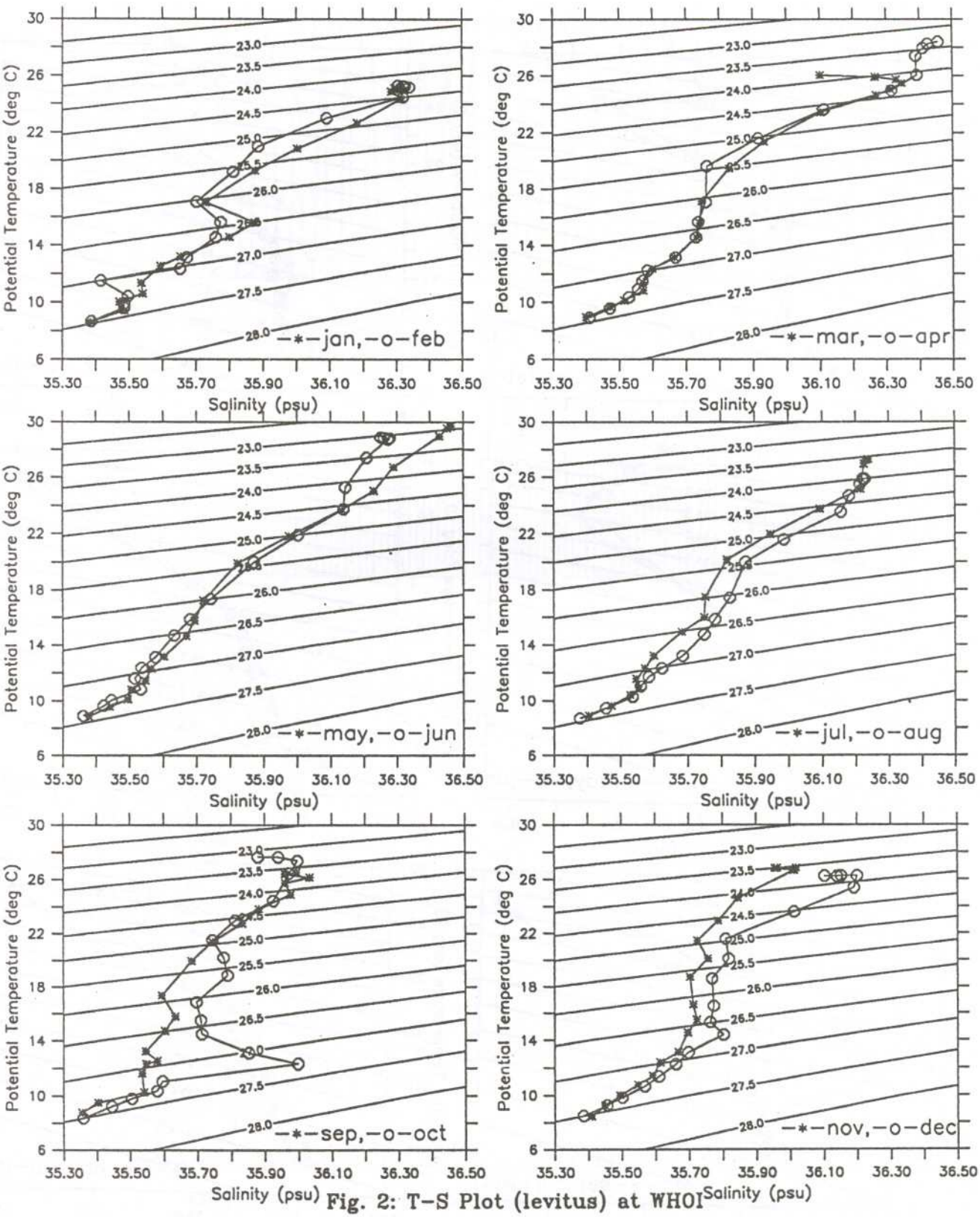


**Fig. 2: T–S Plot (levitus) at WHOI**

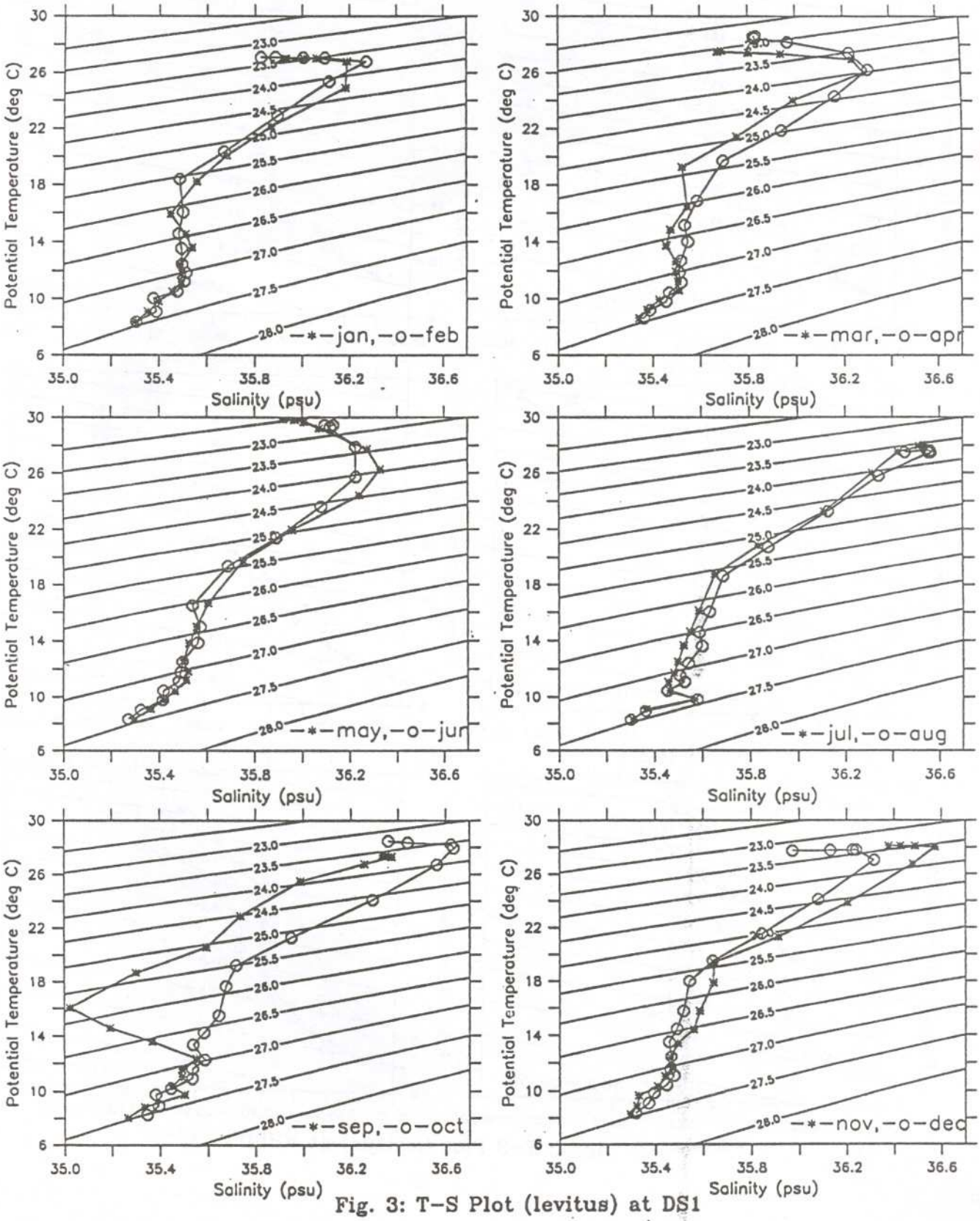


Fig. 3: T–S Plot (levitus) at DS1

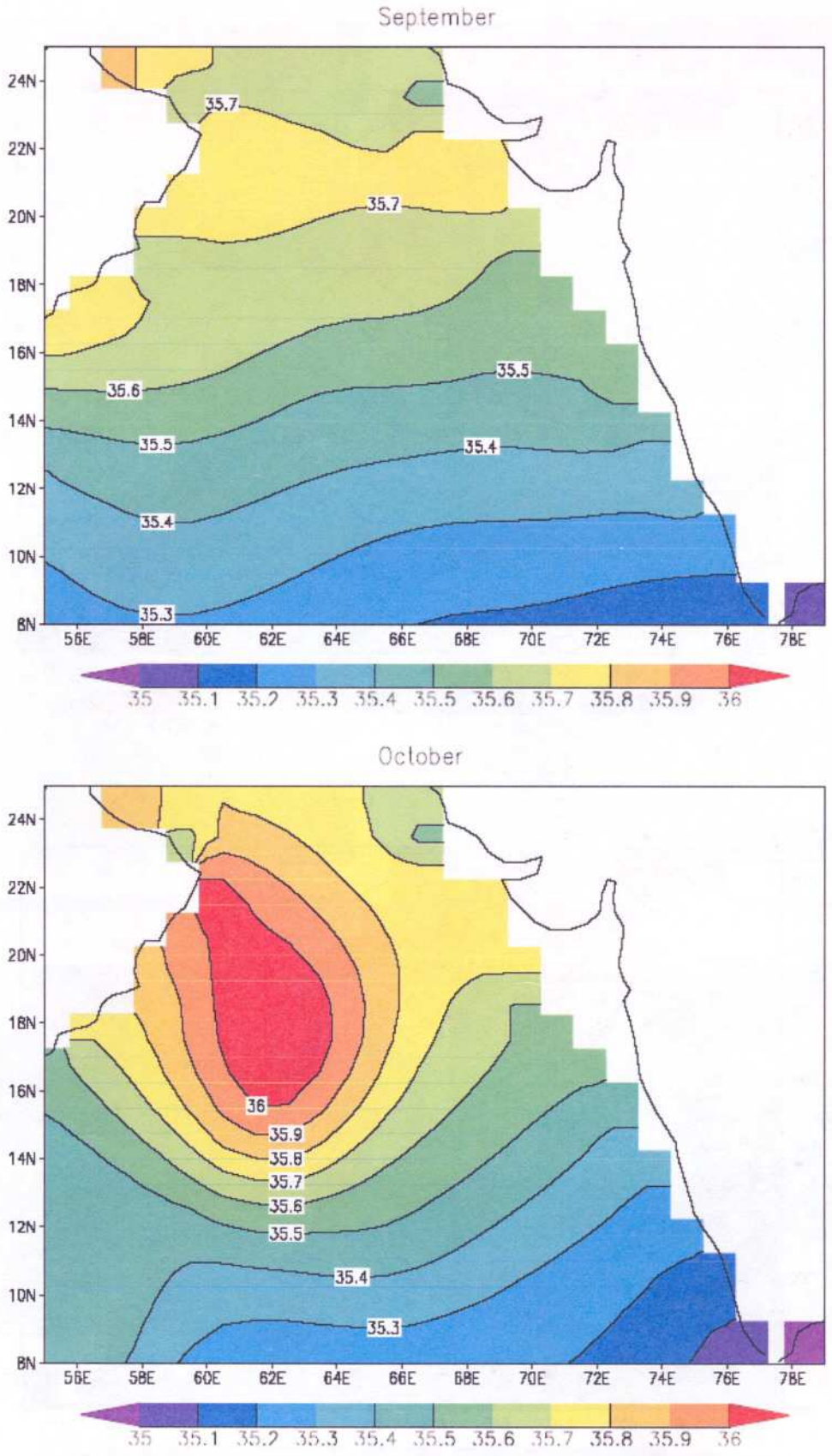


Fig. 4: Levitus climatological Salinity (in psu) at 500 m depth

August

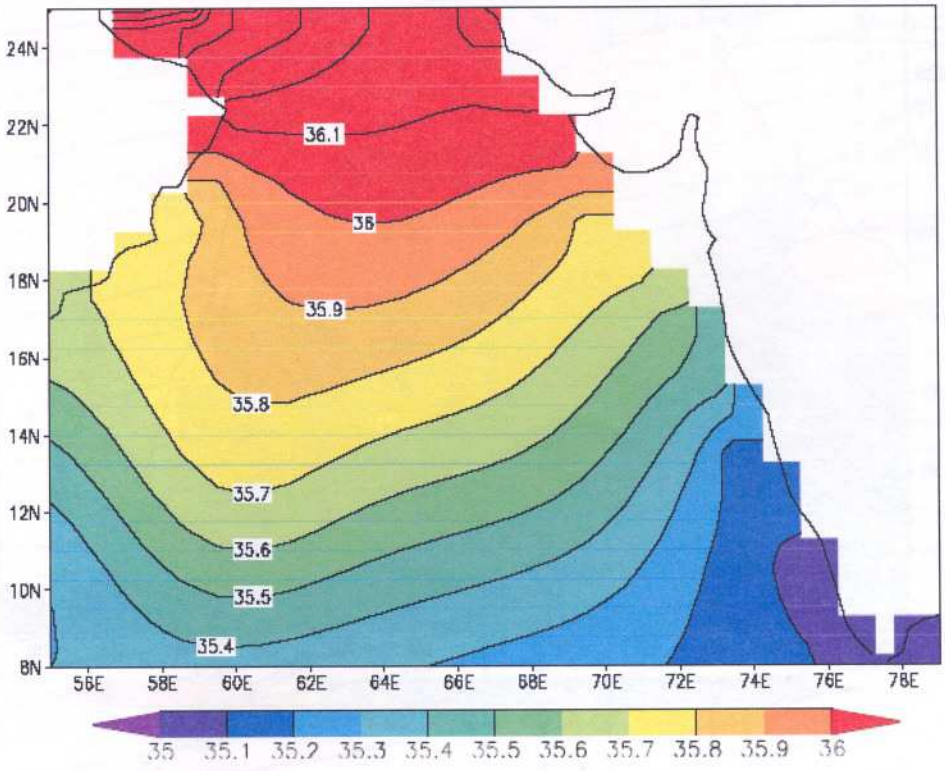


September

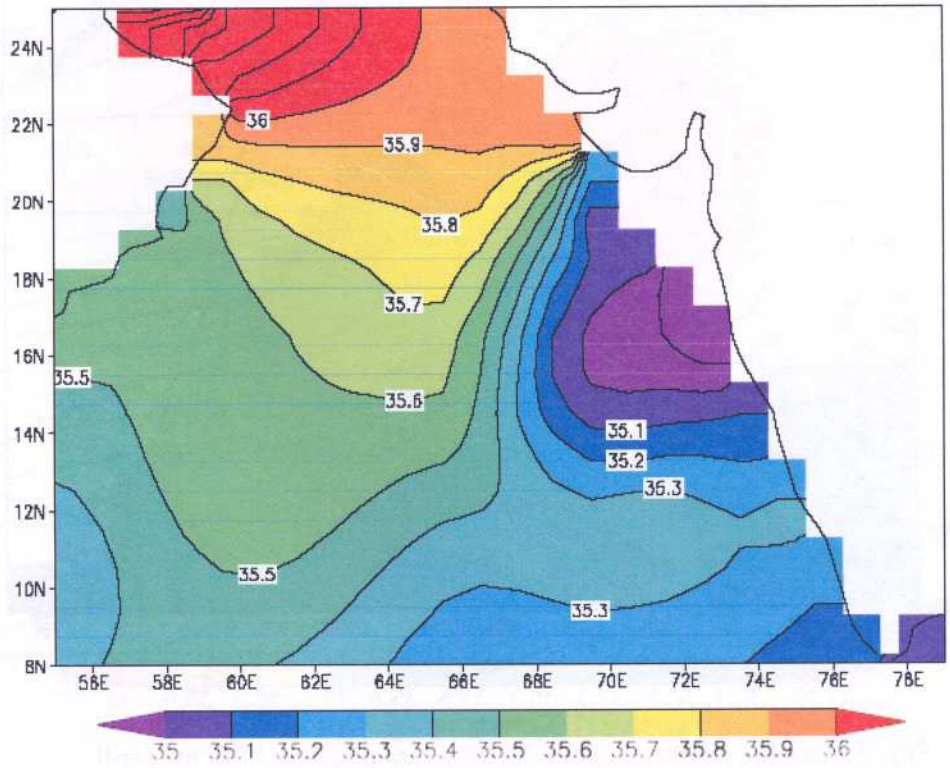


Fig. 5: Levitus climatological Salinity (in psu) at 200 m depth

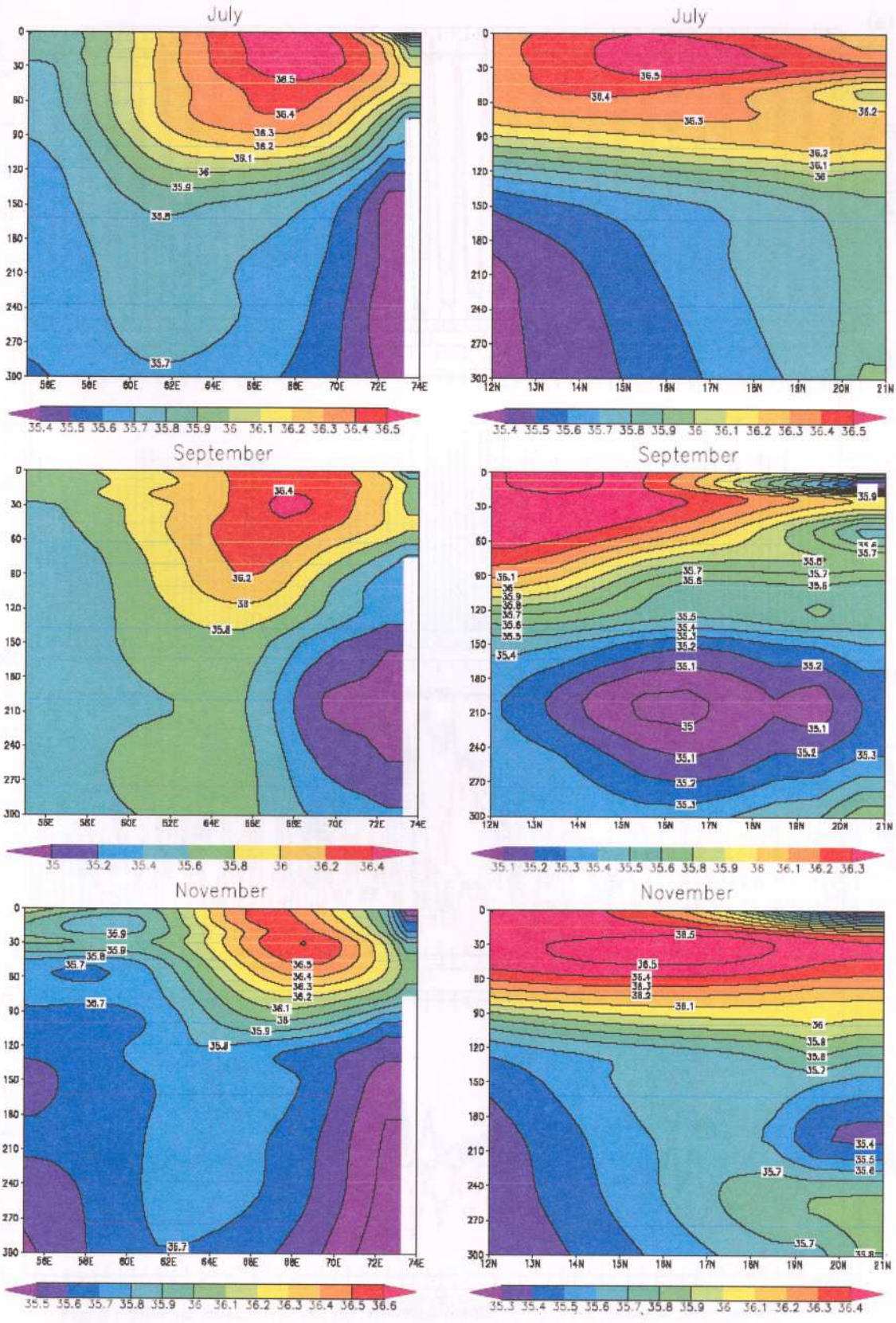


Fig. 6: Vertical section of Levitus climatological Salinity (in psu), left panel shows zonal variation & right panel meridional variation along DS1 point

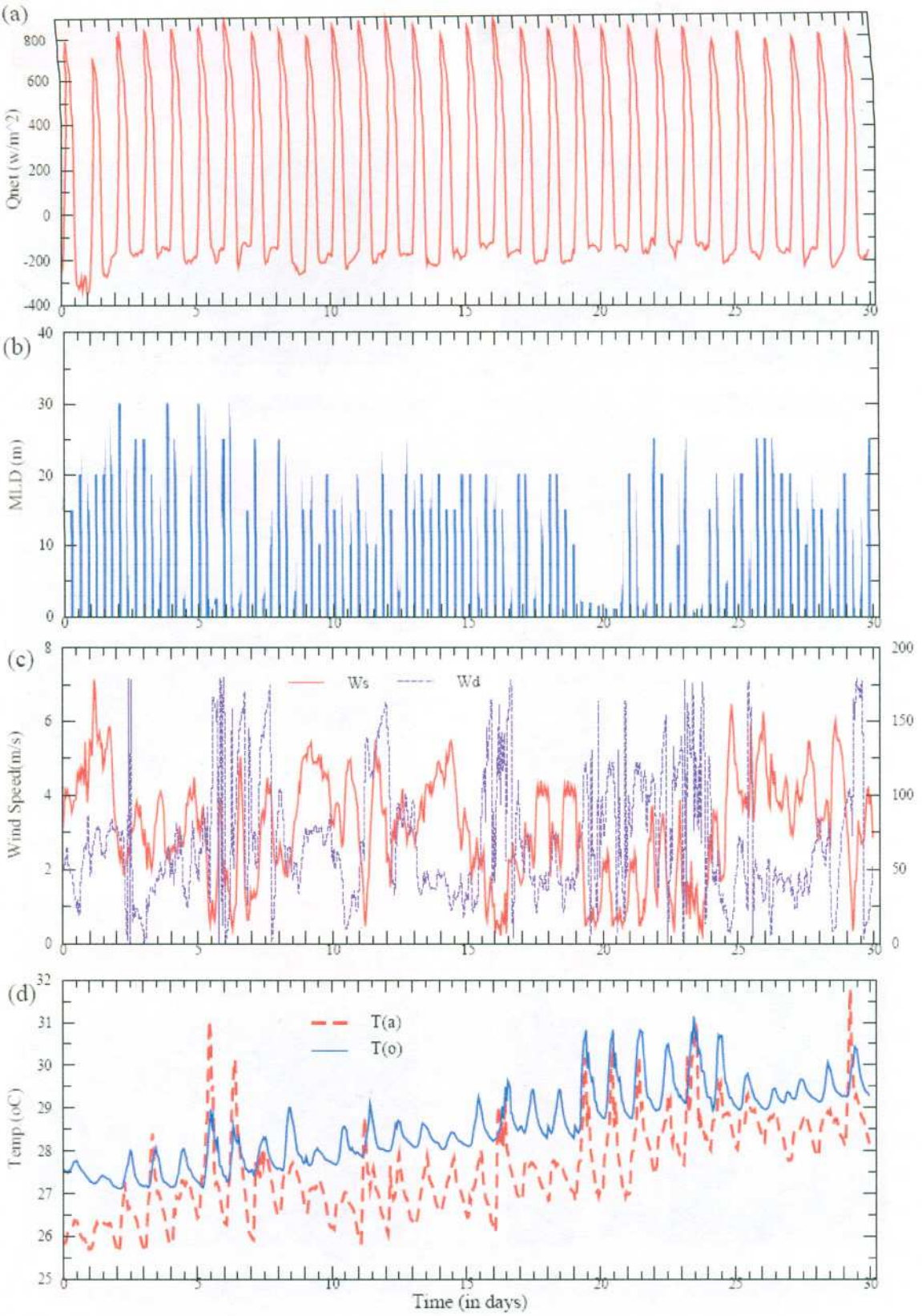


**Fig. 7 : Diurnal variation of (a) Net flux, (b) MLD, (c) Wind Speed & direction and (d) Air temperature & SST at WHOI mooring in April 1995**

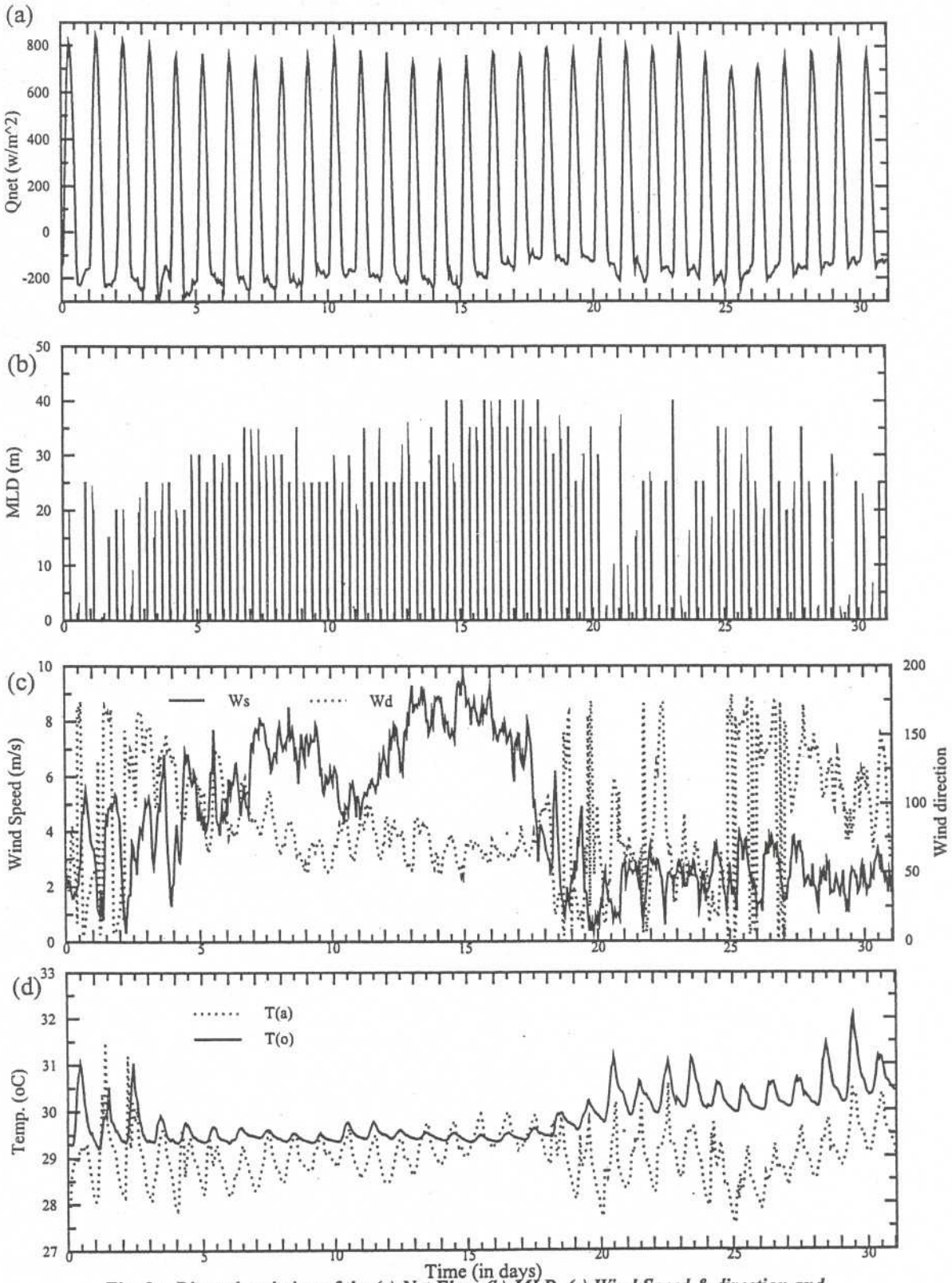


*Fig. 8 : Diurnal variation of the (a) Net Flux, (b) MLD, (c) Wind Speed & direction and (d) Air temperature & SST at WHOI mooring in May 1995*

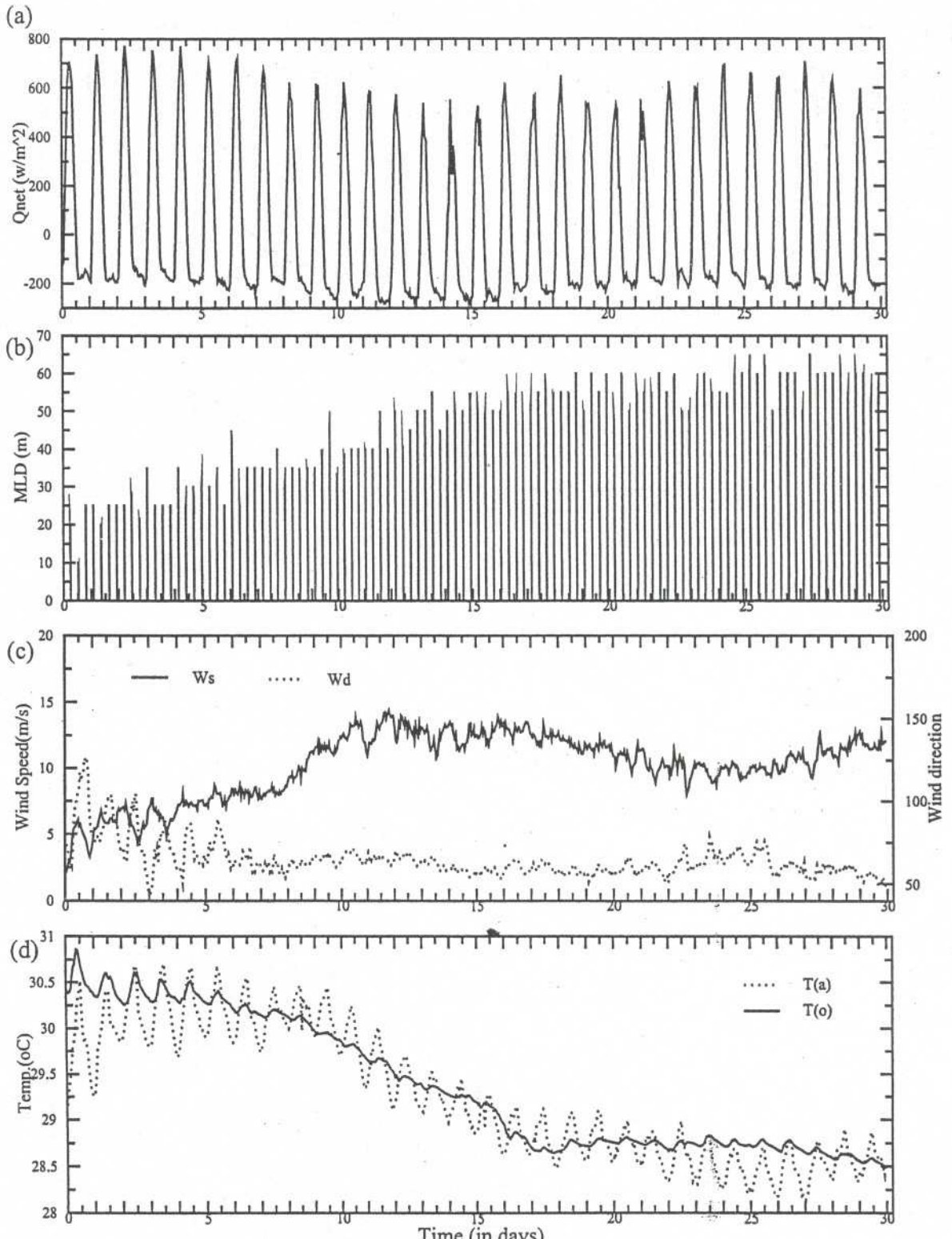


***Fig. 9: Diurnal variation of the (a) Net Flux, (b) MLD, (c) Wind Speed & direction and (d) Air temperature & SST at WHOI mooring in June 1995***

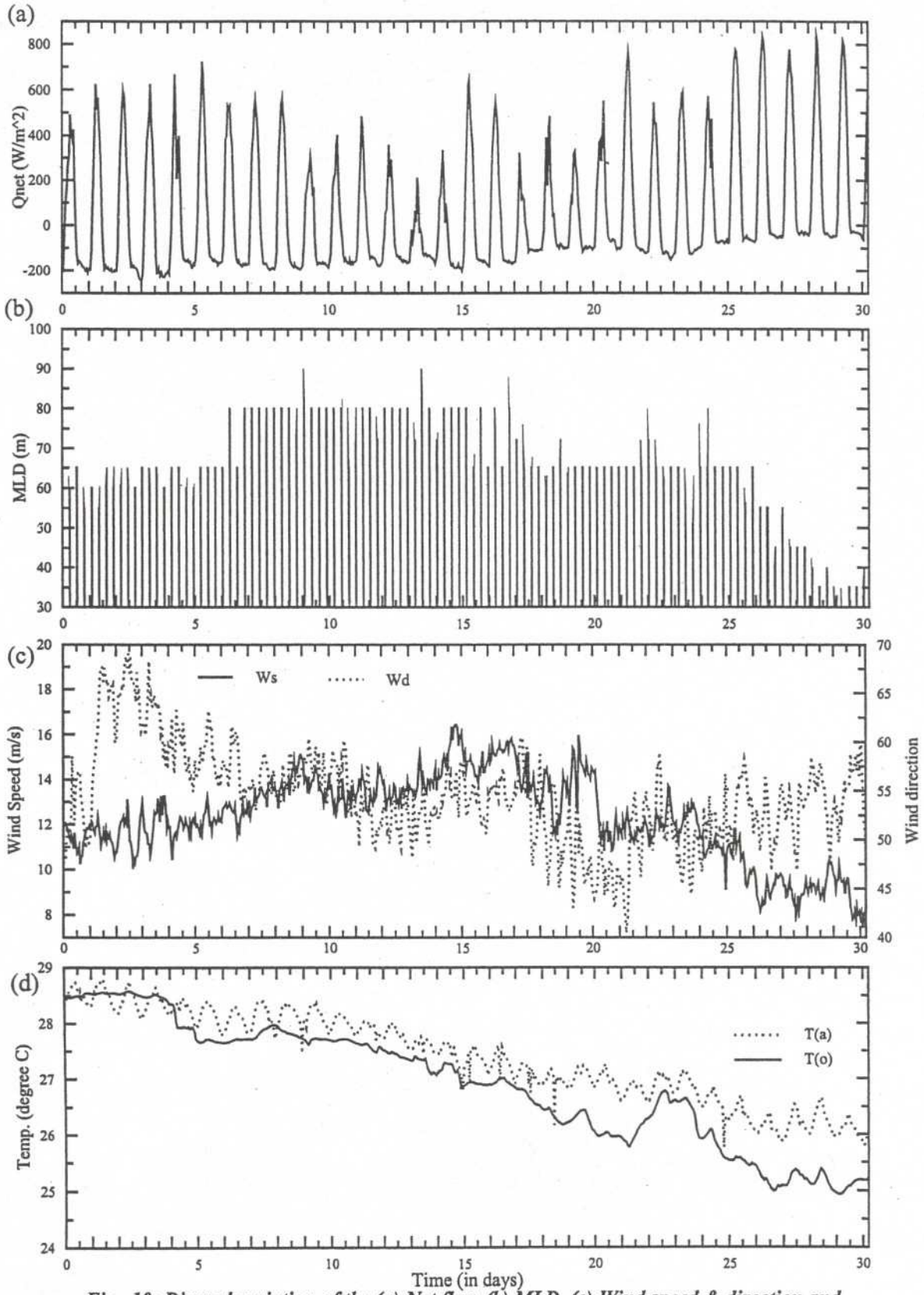


*Fig. 10: Diurnal variation of the (a) Net flux, (b) MLD, (c) Wind speed & direction and (d) Air temperature & SST at WHOI mooring in July 1995*

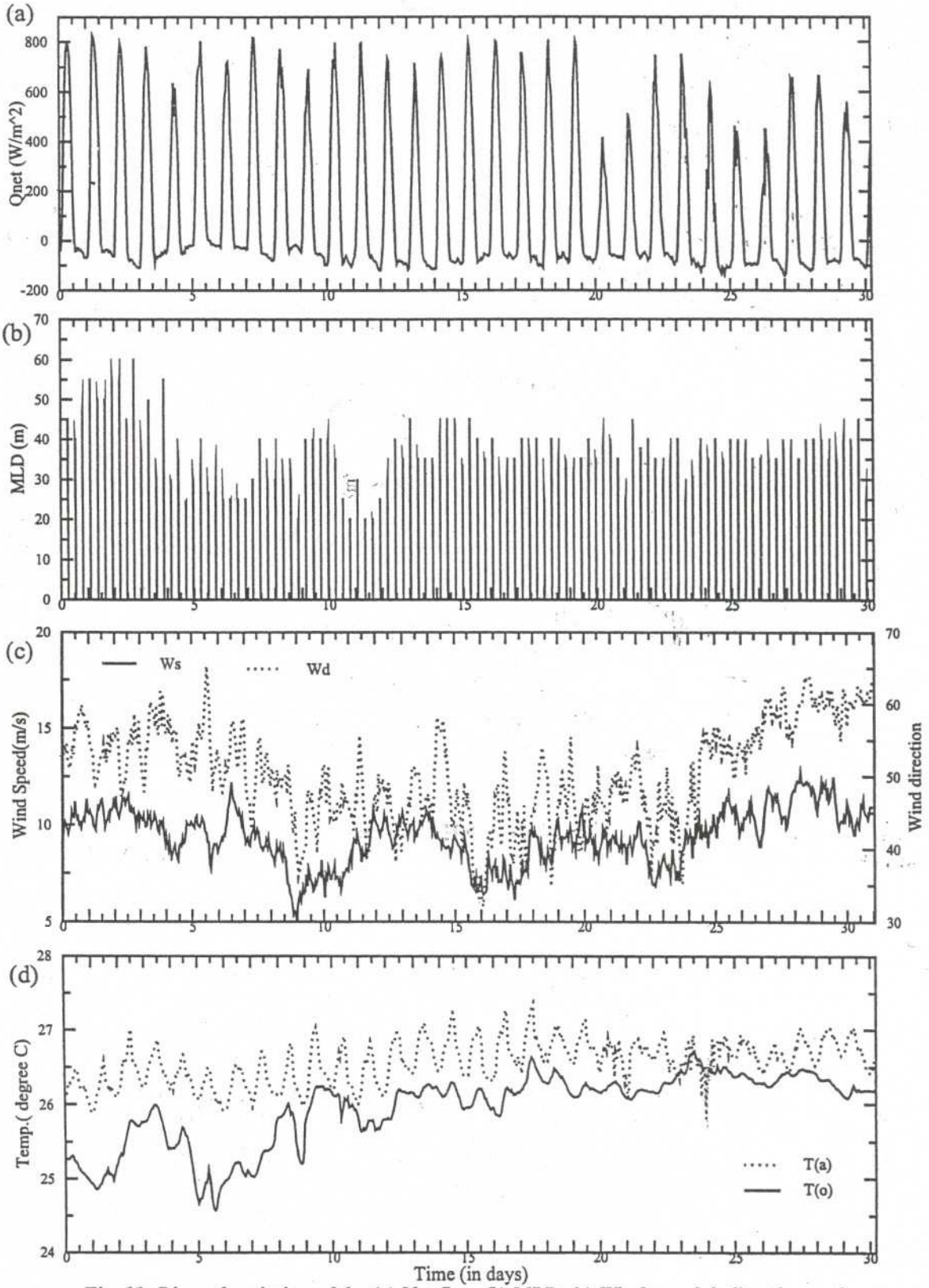


*Fig. 11: Diurnal variation of the (a) Net flux, (b) MLD, (c) Wind speed & direction and (d) Air temperature & SST at WHOI mooring in August 1995*

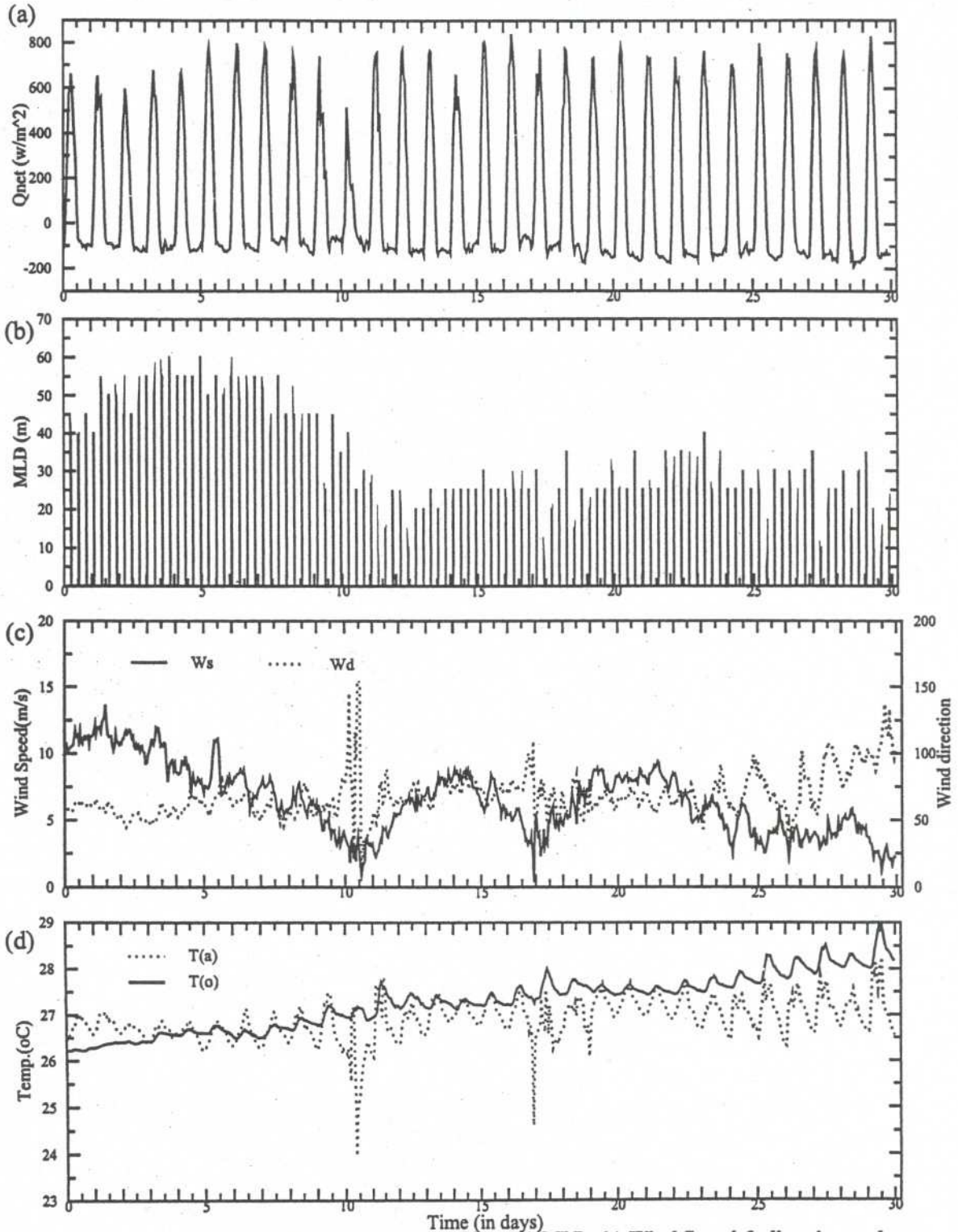


***Fig. 12: Diurnal variation of the (a) Net Flux, (b) MLD, (c) Wind Speed & direction and (d) Air temperature & SST at WHOI mooring in September 1995***

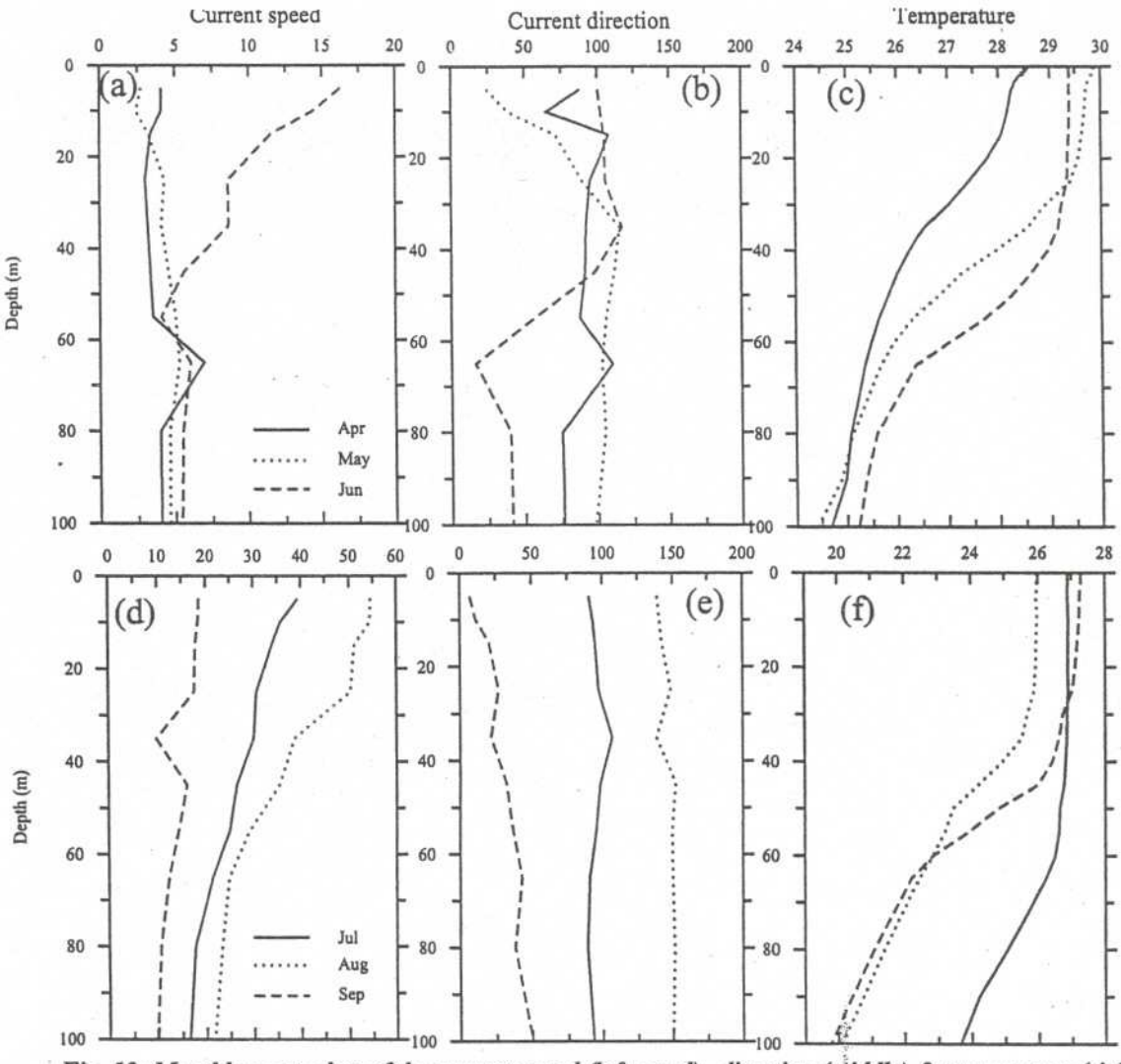


*Fig. 13: Monthly mean plots of the current speed (left panel) , direction (middle) & temperature (right)*

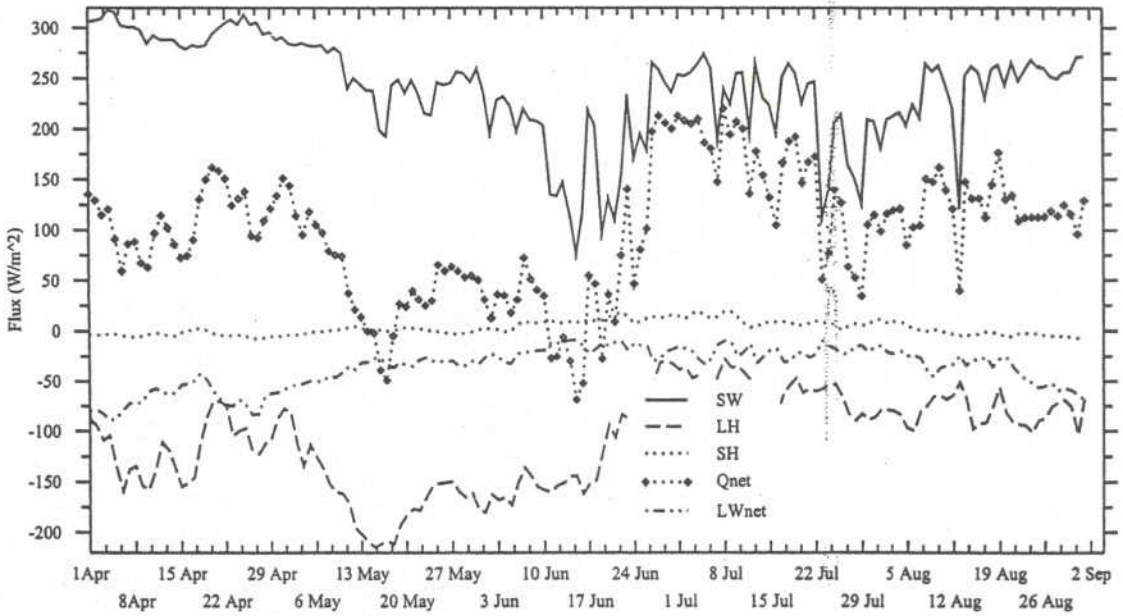


*Fig. 14: Daily mean plots of the air sea fluxes*

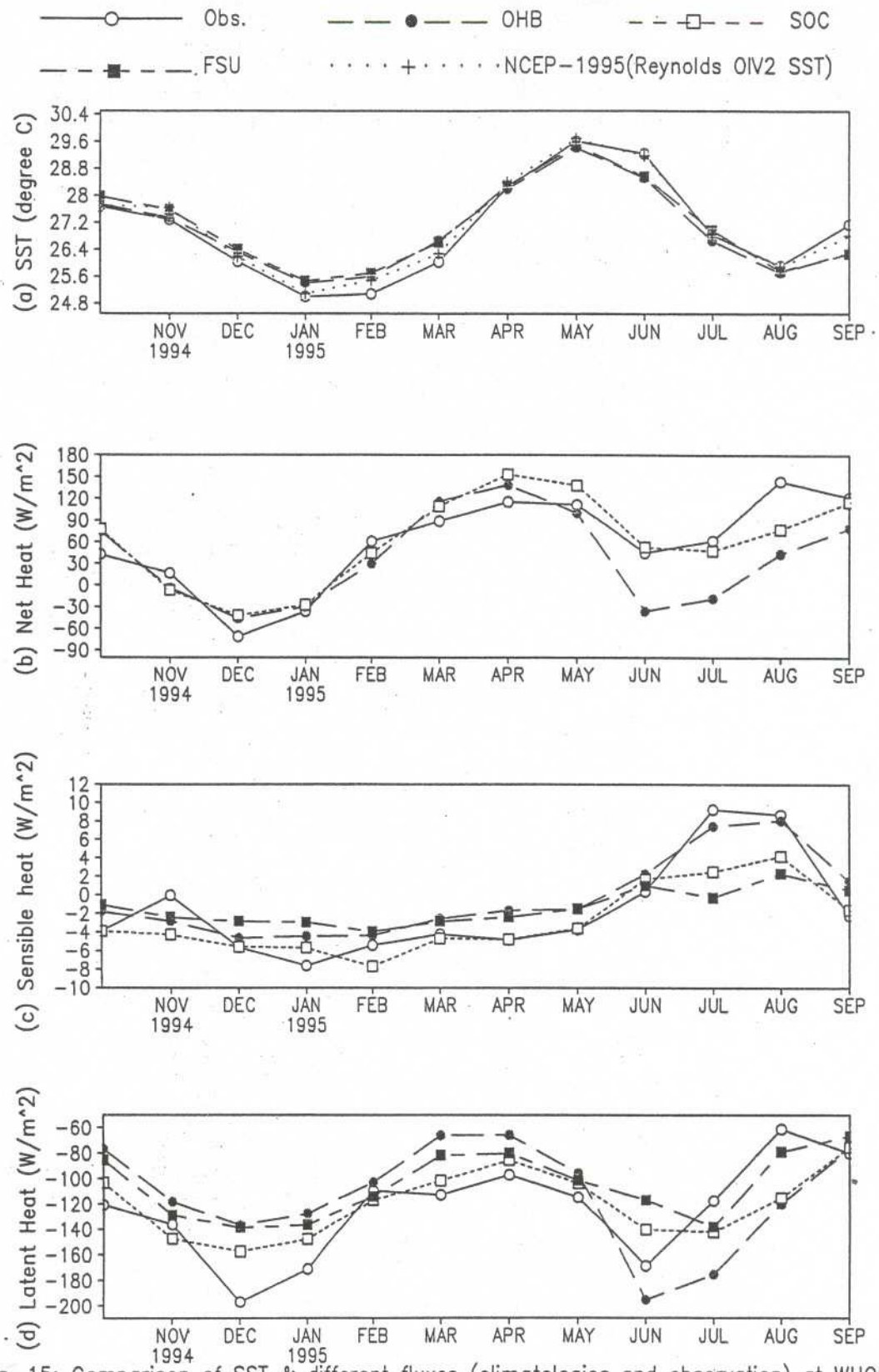


Fig. 15: Comparison of SST & different fluxes (climatologies and observation) at WHOI

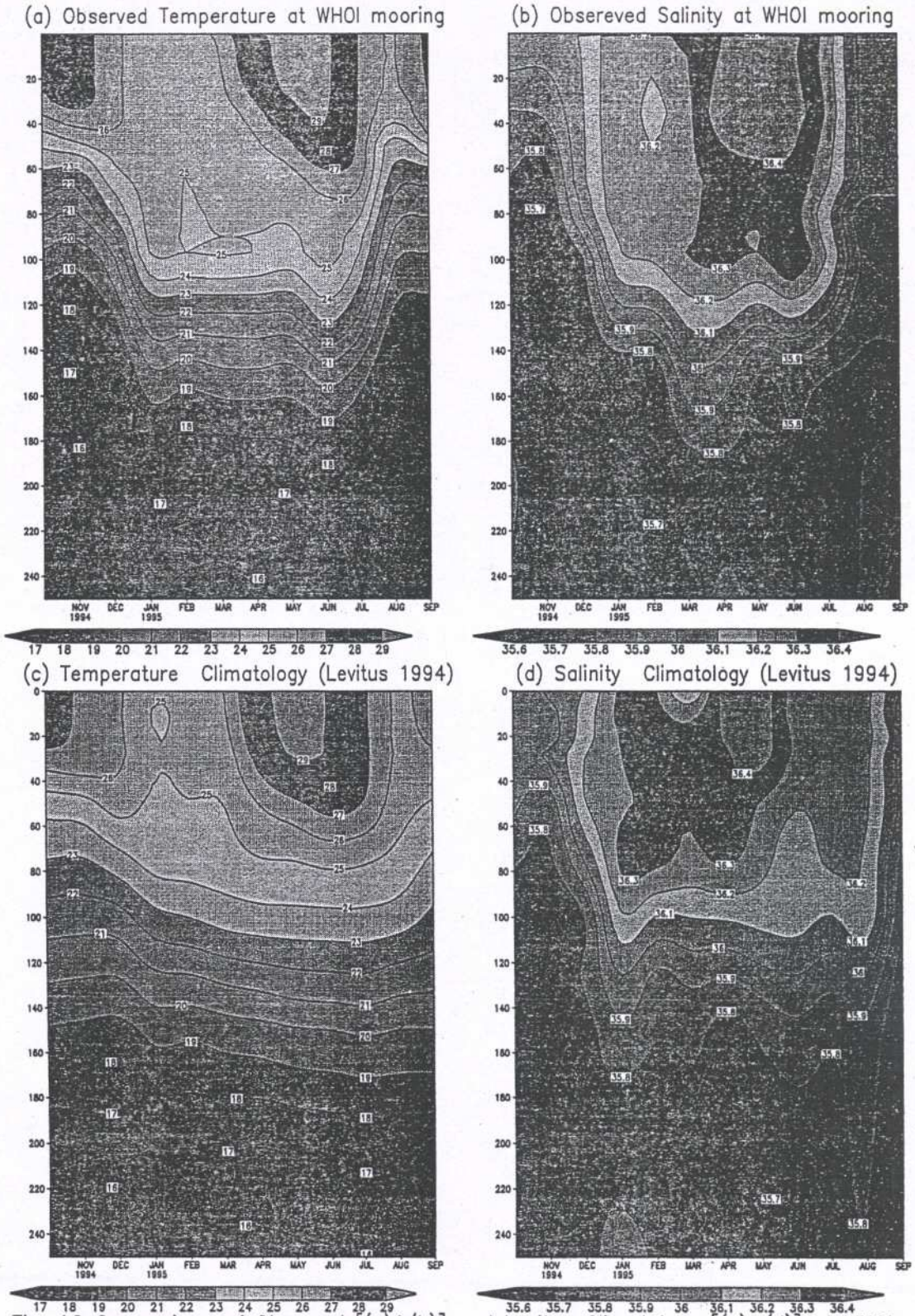


Fig. 16 Comparison of Observed [(a)&(b)] and Levitus Climatology [(c)&(d)] at WHOI

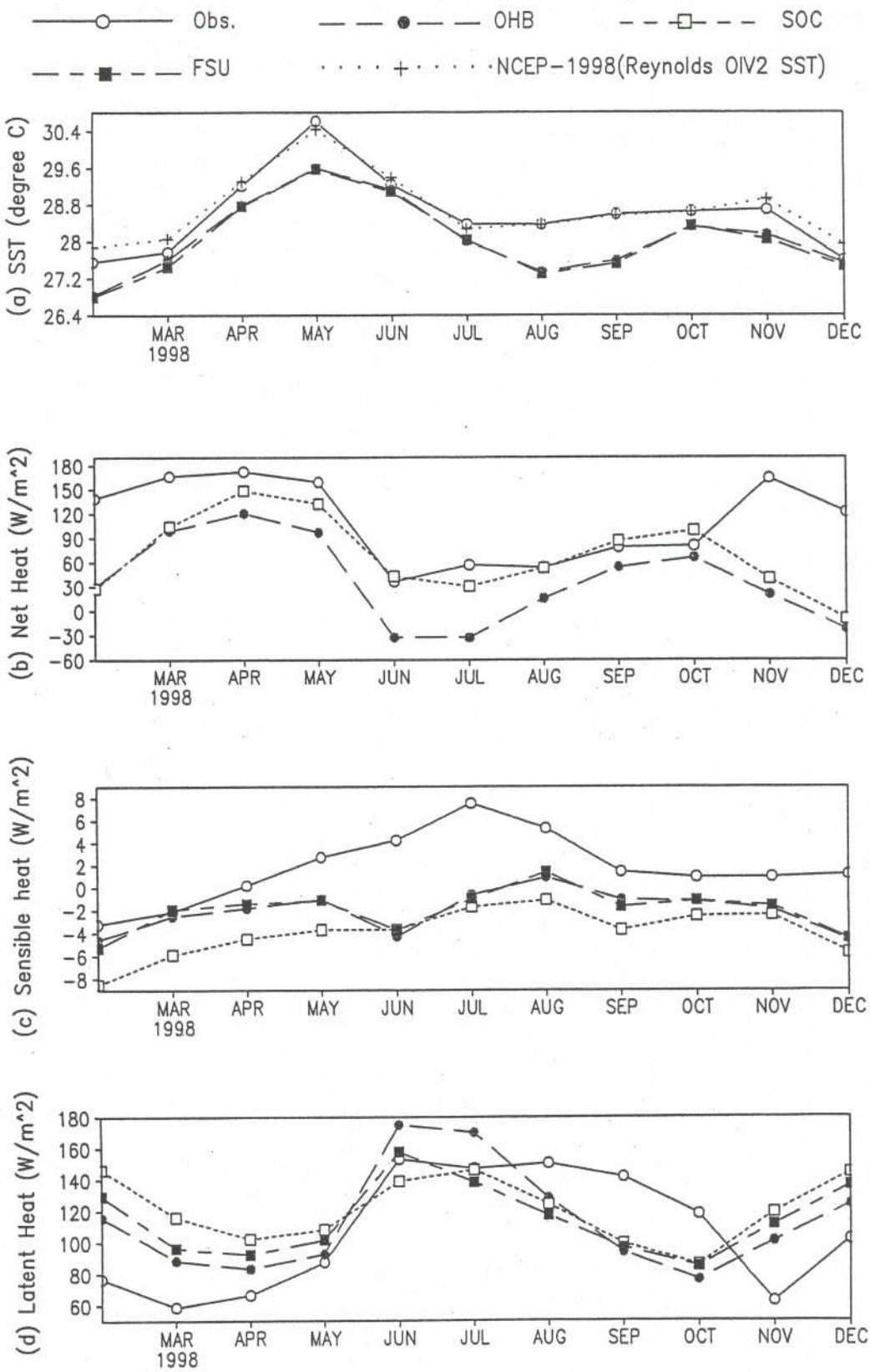


Fig. 17: Comparison of SST & different fluxes (climaologies and Observation) at DS1

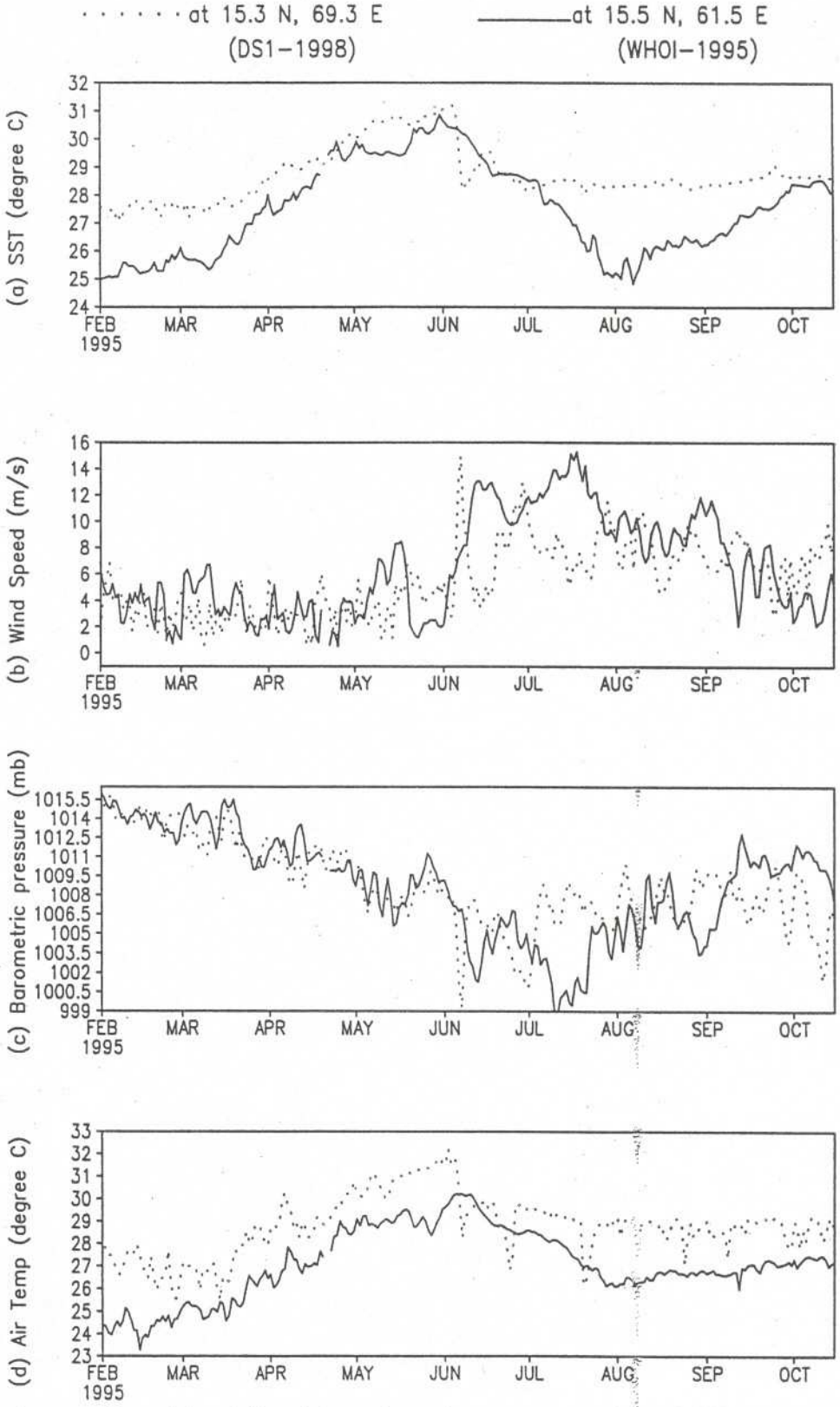


Fig.18 Comparative plots of the daily met. and ocean parameters at WHOI and DS1

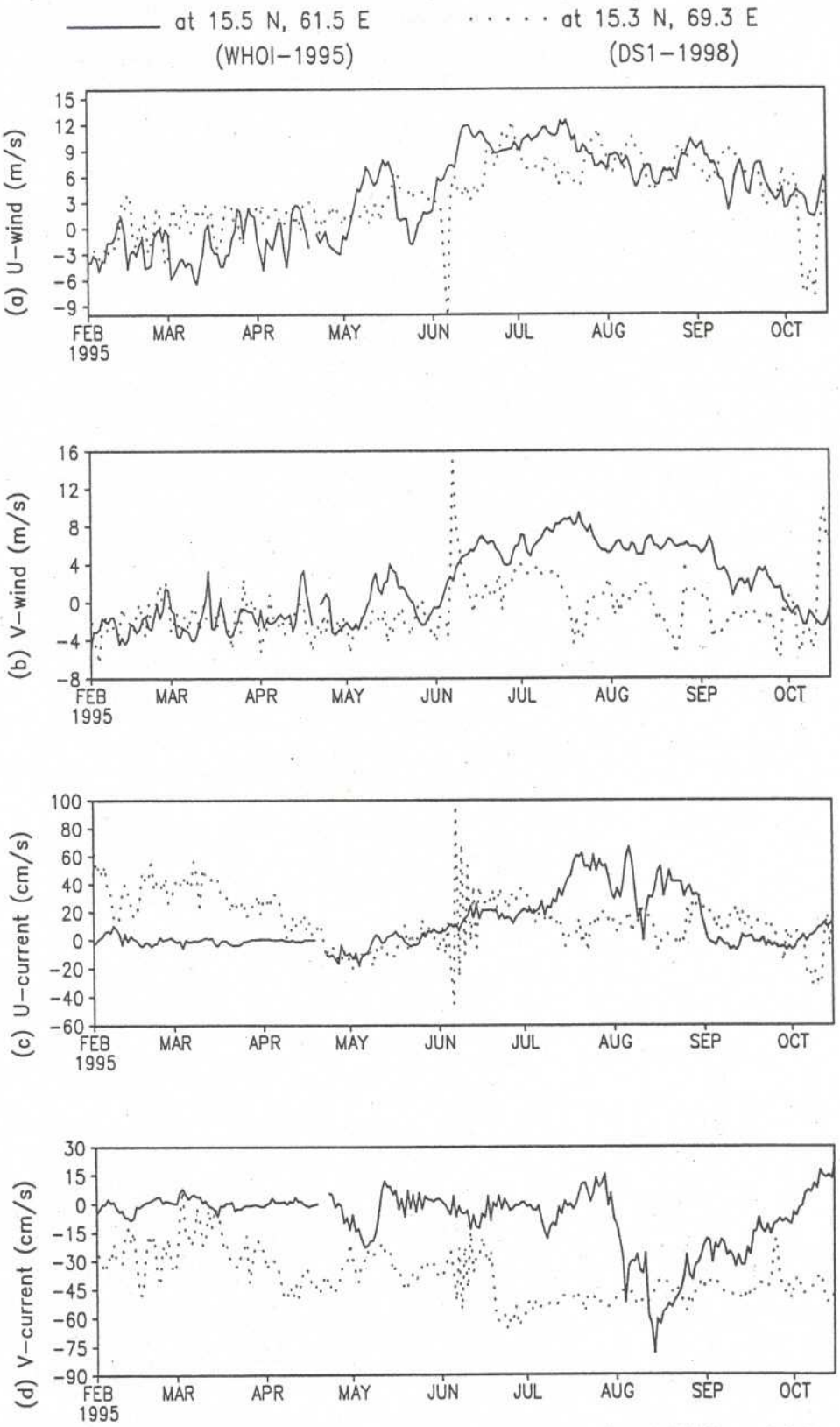


Fig. 19 comparative plots of surface wind and currents at WHOI and DS1

# I. I. T. M. RESEARCH REPORTS

- Energetic consistency of truncated models, *Asnani G.C.*, August 1971, RR-001.
- Note on the turbulent fluxes of heat and moisture in the boundary layer over the Arabian Sea, *Sinha S.*, August 1971, RR-002.
- Simulation of the spectral characteristics of the lower atmosphere by a simple electrical model and using it for prediction, *Sinha S.*, September 1971, RR-003.
- Study of potential evapo-transpiration over Andhra Pradesh, *Rakhecha P.R.*, September 1971, RR-004.
- Climatic cycles in India-1: Rainfall, *Jagannathan P. and Parthasarathy B.*, November 1971, RR-005.
- Tibetan anticyclone and tropical easterly jet, *Raghavan K.*, September 1972, RR-006.
- Theoretical study of mountain waves in Assam, *De U.S.*, February 1973, RR-007.
- Local fallout of radioactive debris from nuclear explosion in a monsoon atmosphere, *Saha K.R. and Sinha S.*, December 1972, RR-008.
- Mechanism for growth of tropical disturbances, *Asnani G.C. and Keshavamurty R.N.*, April 1973, RR-009.
- Note on "Applicability of quasi-geostrophic barotropic model in the tropics", *Asnani G.C.*, February 1973, RR-010.
- On the behaviour of the 24-hour pressure tendency oscillations on the surface of the earth, Part-I: Frequency analysis, Part-II: Spectrum analysis for tropical stations, *Misra B.M.*, December 1973, RR-011.
- On the behaviour of the 24 hour pressure tendency oscillations on the surface of the earth, Part-III : Spectrum analysis for the extra-tropical stations, *Misra B.M.*, July 1976, RR-011A.
- Dynamical parameters derived from analytical functions representing Indian monsoon flow, *Awade S.T. and Asnani G.C.*, November 1973, RR-012.
- Meridional circulation in summer monsoon of Southeast Asia, *Asnani G.C.*, November 1973, RR-014.
- Energy conversions during weak monsoon, *Keshavamurty R.N. and Awade S.T.*, August 1974, RR-015.
- Vertical motion in the Indian summer monsoon, *Awade S.T. and Keshavamurty R.N.*, August 1974, RR-016.
- Semi-annual pressure oscillation from sea level to 100mb in the northern hemisphere, *Asnani G.C. and Verma R.K.*, August 1974, RR-017.
- Suitable tables for application of gamma probability model to rainfall, *Mooley D.A.*, November 1974, RR-018.

- Annual and semi-annual thickness oscillation in thenorthern hemisphere, *Asnani G.C. and Verma R.K.*, January 1975, RR-020.

- Spherical harmonic analysis of the normal constant pressure charts in the northern hemisphere, *Awade S.T., Asnani G.C. and Keshavamurty R.N.*, May 1978, RR-021.

- Dynamical parameters derived from analytical function representing normal July zonal flow along 87.5 °E, *Awade S.T. and Asnani G.C.*, May 1978, RR-022.

- Study of trends and periodicities in the seasonal and annual rainfall of India, *Parthasarathy B. and Dhar O.N.*, July 1975, RR-023.

- Southern hemisphere influence on Indian rainfall, *Raghavan K.., Paul D.K. and Upasani P.U.*, February 1976, RR-024.

- Climatic fluctuations over Indian region - Rainfall : A review, *Parthasarathy B. and Dhar O.N.*, May 1978, RR-025.

- Annual variation of meridional flux of sensible heat, *Verma R.K. and Asnani G.C.*, December 1978, RR-026.

- Poisson distribution and years of bad monsoon over India, *Mooley D.A and Parthasarathy B.*, April 1980, RR-027.

- On accelerating the FFT of Cooley and Tukey, *Mishra S.K.*, February 1981, RR-028.

- Wind tunnel for simulation studies of the atmospheric boundary layer, *Sivaramakrishnan S.*, February 1981, RR-029.

- Hundred years of Karnataka rainfall, *Parthasarathy B. and Mooley D.A.*, March 1981, RR-030.

- Study of the anomalous thermal and wind patterns during early summer season of 1979 over the Afro-Asian region in relation to the large-scale performance of the monsoon over India, *Verma R.K. and Sikka D.R.*, March 1981, RR-031.

- Some aspects of oceanic ITCZ and its disturbances during the onset and established phase of summer monsoon studied with Monex-79 data, *Sikka D.R., Paul D.K. and Singh S.V.*, March 1981, RR- 032.

- Modification of Palmer drought index, *Bhalme H.N. and Mooley D.A.*, March 1981, RR-033.

- Meteorological rocket payload for Menaka-II/Rohini 200 and its developmental details, *Vernekar K.G. and Brij Mohan*, April 1981, RR-034.

- Harmonic analysis of normal pentad rainfall of Indian stations, *Anathakrishnan R. and Pathan J.M.*, October 1981, RR-035.

- Pentad rainfall charts and space-time variations of rainfall over India and the adjoining areas, *Anathakrishnan R. and Pathan J.M.*, November 1981, RR-036.

- Dynamic effects of orography on the large scale motion of the atmosphere Part I : Zonal flow and elliptic barrier with maximum height of one km., *Bavadekar S.N. and Khaladkar R.M.*, January 1983, RR-037.

- Limited area five level primitive equation model, *Singh S.S.*, February 1983, RR-038.
- Developmental details of vortex and other aircraft thermometers, *Vernekar K.G., Brij Mohan and Srivastava S.*, November 1983, RR-039.
- Note on the preliminary results of integration of a five level P.E. model with westerly wind and low orography, *Bavadekar S.N., Khaladkar R.M., Bandyopadhyay A. and Seetaramayya P.*, November 1983, RR-040.
- Long-term variability of summer monsoon and climatic change, *Verma R.K., Subramaniam K. and Dugam S.S.*, December 1984, RR-041.
- Project report on multidimensional initialization for NWP models, *Sinha S.*, February 1989, RR-042.
- Numerical experiments with inclusion of orography in five level P.E. Model in pressure-coordinates for interhemispheric region, *Bavadekar S.N. and Khaladkar R.M.*, March 1989, RR-043.
- Application of a quasi-lagrangian regional model for monsoon prediction, *Singh S.S. and Bandyopadhyay A.*, July 1990, RR-044.
- High resolution UV-visible spectrometer for atmospheric studies, *Bose S., Trimbake H.N., Londhe A.L. and Jadhav D.B.*, January 1991, RR-045.
- Fortran-77algorithm for cubic spline interpolation for regular and irregular grids, *Tandon M.K.*, November 1991, RR-046.
- Fortran algorithm for 2-dimensional harmonic analysis, *Tandon M.K.*, November 1991, RR- 047.
- 500 hPa ridge and Indian summer monsoon rainfall : A detailed diagnostic study, *Krishna Kumar K., Rupa Kumar K. and Pant G.B.*, November 1991, RR-048.
- Documentation of the regional six level primitive equation model, *Singh S.S. and Vaidya S.S.*, February 1992, RR-049.
- Utilisation of magnetic tapes on ND-560 computer system, *Kripalani R.H. and Athale S.U.*, July 1992, RR-050.
- Spatial patterns of Indian summer monsoon rainfall for the period 1871-1990, *Kripalani R.H., Kulkarni A.A., Panchawagh N.V. and Singh S.V.*, August 1992, RR-051.
- FORTRAN algorithm for divergent and rotational wind fields, *Tandon M.K.*, November 1992, RR-052.
- Construction and analysis of all-India summer monsoon rainfall series for the longest instrumental period: 1813-1991, *Sontakke N.A., Pant G.B. and Singh N.*, October 1992, RR-053.
- Some aspects of solar radiation, *Tandon M.K.*, February 1993, RR-054.
- Design of a stepper motor driver circuit for use in the moving platform, *Dharmaraj T. and Vernekar K.G.*, July 1993, RR-055.

- Experimental set-up to estimate the heat budget near the land surface interface, *Vernekar K.G., Saxena S., Pillai J.S., Murthy B.S., Dharmaraj T. and Brij Mohan,* July 1993, RR-056.

- Identification of self-organized criticality in atmospheric total ozone variability, *Selvam A.M. and Radhamani M.,* July 1993, RR-057.

- Deterministic chaos and numerical weather prediction, *Selvam A.M.,* February 1994, RR-058.

- Evaluation of a limited area model forecasts, *Singh S.S., Vaidya S.S Bandyopadhyay A., Kulkarni A.A, Bawiskar S.M., Sanjay J., Trivedi D.K. and Iyer U.,* October 1994, RR-059.

- Signatures of a universal spectrum for atmospheric interannual variability in COADS temperature time series, *Selvam A.M., Joshi R.R. and Vijayakumar R.,* October 1994, RR-060.

- Identification of self-organized criticality in the interannual veriability of global surface temperature, *Selvam A.M. and Radhamani M.,* October 1994, RR-061.

- Identification of a universal spectrum for nonlinear veriability of solar-geophysical parameters, *Selvam A.M., Kulkarni M.K., Pethkar J.S. and Vijayakumar R.,* October 1994, RR-062.

- Universal spectrum for fluxes of energetic charged particles from the earth's magnetosphere, *Selvam A.M. and Radhamani M.,* June 1995, RR-063.

- Estimation of nonlinear kinetic energy exchanges into individual triad interactions in the frequency domain by use of the cross-spectral technique, *Chakraborty D.R.,* August 1995, RR-064.

- Monthly and seasonal rainfall series for all-India homogeneous regions and meteorological subdivisions: 1871-1994, *Parthasarathy B., Munot A.A. and Kothawale D.R.,* August 1995, RR-065.

- Thermodynamics of the mixing processes in the atmospheric boundary layer over Pune during summer monsoon season, *Morwal S.B. and Parasnis S.S.,* March 1996, RR-066.

- Instrumental period rainfall series of the Indian region: A documentation, *Singh N. and Sontakke N.A.,* March 1996, RR-067.

- Some numerical experiments on roundoff-error growth in finite precision numerical computation, *Fadnavis S.,* May 1996, RR-068.

- Fractal nature of MONTBLEX time series data, *Selvam A.M. and Sapre V.V.,* May 1996, RR-069.

- Homogeneous regional summer monsoon rainfall over India: Interannual variability and teleconnections, *Parthasarathy B., Rupa Kumar K. and Munot A.A.,* May 1996, RR-070.

- Universal spectrum for sunspot number variability, *Selvam A.M. and Radhamani M.,* November 1996, RR-071.

- Development of simple reduced gravity ocean model for the study of upper north Indian ocean, *Behera S.K. and Salvekar P.S.*, November 1996, RR-072.

- Study of circadian rhythm and meteorological factors influencing acute myocardial infraction, *Selvam A.M., Sen D. and Mody S.M.S.*, April 1997, RR-073.

- Signatures of universal spectrum for atmospheric gravity waves in southern oscillation index time series, *Selvam A.M., Kulkarni M.K., Pethkar J.S. and Vijayakumar R.*, December 1997, RR-074.

- Some example of X-Y plots on Silicon Graphics, *Selvam A.M., Fadnavis S. and Gharge S.P.*, May 1998, RR-075.

- Simulation of monsoon transient disturbances in a GCM, *Ashok K., Soman M.K. and Satyan V.*,August 1998, RR-076.

- Universal spectrum for intraseasonal variability in TOGA temperature time series, *Selvam A.M., Radhamani M., Fadnavis S. and Tinmaker M.I.R.*, August 1998, RR-077.

- One dimensional model of atmospheric boundary layer, *Parasnis S.S., Kulkarni M.K., Arulraj S. and Vernekar K.G.*, February 1999, RR-078.

- Diagnostic model of the surface boundary layer - A new approach, *Sinha S.*, February 1999, RR-079.

- Computation of thermal properties of surface soil from energy balance equation using force - restore method, *Sinha S.*, February 1999, RR-080.

- Fractal nature of TOGA temperature time series, *Selvam A.M. and Sapre V.V.*, February 1999, RR-081.

- Evolution of convective boundary layer over the Deccan Plateau during summer monsoon, *Parasnis S.S.*, February 1999, RR-082.

- Self-organized criticality in daily incidence of acute myocardial infarction, *Selvam A.M., Sen D., and Mody S.M.S.*, Feburary 1999, RR-083.

- Monsoon simulation of 1991 and 1994 by GCM : Sensitivity to SST distribution, *Ashrit R.G., Mandke S.K. and Soman M.K.*, March 1999, RR-084.

- Numerical investigation on wind induced interannual variability of the north Indian Ocean SST, *Behera S.K., Salvekar P.S. and Ganer D.W.*, April 1999, RR-085.

- On step mountain eta model, *Mukhopadhyay P., Vaidya S.S., Sanjay J. and Singh S.S.*, October 1999, RR-086.

- Land surface processes experiment in the Sabarmati river basin: an overview and early results, *Vernekar K.G., Sinha S., Sadani L.K., Sivaramakrishnan S., Parasnis S.S., Brij Mohan, Saxena S., Dharamraj T., Pillai, J.S., Murthy B.S., Debaje, S.B., Patil, M.N. and Singh A.B.*, November 1999, RR-087.

- Reduction of AGCM systematic error by Artificial Neural Network: A new approach for dynamical seasonal prediction of Indian summer monsoon rainfall, *Sahai A.K. and Satyan V.*, December 2000, RR-088.

- Ensemble GCM simulations of the contrasting Indian summer monsoons of the 1987 and 1988, Mujumdar M. and Krishnan R., February 2001, RR-089.

- Aerosol measurements using lidar and radiometers at Pune during INDOEX field phases, Maheskumar R.S., Devara P.C.S., Raj P.E., Jaya Rao Y.,Pandithurai G., Dani K.K., Saha S.K., Sonbawne S.M. and Tiwari Y.K., December 2001, RR-090.

- Modelling studies of the 2000 Indian summer monsoon and extended analysis, Krishnan R., Mujumdar M., Vaidya V., Ramesh K.V. and Satyan V., December 2001, RR-091.

- Intercomparison of Asian summer monsoon 1997 simulated by atmospheric general circulation models, Mandke S.K., Ramesh K.V. and Satyan V., December 2001, RR-092.

- Prospects of prediction of Indian summer monsoon rainfall using global SST anomalies, Sahai A.K, Grimm A.M., Satyan V. and Pant G.B., April 2002, RR-093.

- Estimation of nonlinear heat and momentum transfer in the frequency domain buy the use of frequency co-spectra and cross-bispectra, Chakraborty D.R. and Biswas M.K., August 2002, RR-094

- Real time simulations of surface circulations by a simple ocean model, P Rahul Chand Reddy, Salvekar P.S., Ganer D.W. and Deo A.A., January 2003, RR-095

- Evidence of twin gyres in the Indian ocean : new insights using reduced gravity model by daily winds, P Rahul Chand Reddy, Salvekar P.S., Ganer D.W. and Deo A.A., February 2003, RR-096

- Dynamical seasonal prediction experiments of the Indian summer monsoon, Milind Mujumdar, R. Krishnan and V. Satyan, June 2003, RR-097